

## Core excitations in $^{63}\text{Cu}$ by the $^{63}\text{Cu}(p,p')^{63}\text{Cu}$ and $^{65}\text{Cu}(p,t)^{63}\text{Cu}$ reactions

Y. Iwasaki,\* G. M. Crawley, and J. E. Finck

Cyclotron Laboratory, Michigan State University, East Lansing, Michigan 48824

(Received 30 December 1980)

Core excitations up to  $E_x = 4$  MeV in  $^{63}\text{Cu}$  have been studied by the reactions  $^{63}\text{Cu}(p,p')^{63}\text{Cu}$  and  $^{65}\text{Cu}(p,t)^{63}\text{Cu}$  at 40 MeV proton energy. The transferred angular momentum  $L$  has been determined for each transition on the basis of the angular distribution shape. A quartet-plus-doublet pattern is consistently observed for the groups of states corresponding to the  $2_1^+$ ,  $3_1^-$ , and  $4_1^+$  states of the core nucleus  $^{62}\text{Ni}$ . This implies the existence of doublets arising from the coupling of collective states of the core with the  $2p_{1/2}$  proton orbital, in addition to the quartets from the coupling with the  $2p_{3/2}$  proton orbital considered in the conventional weak-coupling excited-core model. It is pointed out that the existence of a weak-coupling situation cannot be proved only on the basis of transfer-reaction data, and in this regard the importance of a comparative study of the inelastic-scattering and transfer-reaction data is emphasized.

NUCLEAR REACTIONS  $^{65}\text{Cu}(p,t)^{63}\text{Cu}$  and  $^{63}\text{Cu}(p,p')^{63}\text{Cu}$ ,  $E = 40$  MeV; measured  $E_x$  and  $\sigma(\theta)$ , determined  $L$ . Resolution 16 keV for the  $(p,t)$ , 20 keV for the  $(p,p')$ . Enriched targets. Deduced excited-core multiplets.

### I. INTRODUCTION

Low-lying states in a number of spherical, odd nuclei have been interpreted in terms of the particle- (hole-) core-coupling picture<sup>1,2</sup> or the particle- (hole-) vibration-coupling picture.<sup>3,4</sup> The nucleus  $^{63}\text{Cu}$  is a typical example of such nuclei. In the particle-core-coupling picture, the nucleus  $^{63}\text{Cu}$  consists of one proton added to the proton-closed-shell nucleus  $^{62}\text{Ni}$  which is called the core.<sup>2,5</sup> Inelastic scattering has been shown to be an effective means of selectively exciting collective degrees of freedom of the core.<sup>6-9</sup> More recently, the  $^{65}\text{Cu}(p,t)^{63}\text{Cu}$  reaction was used to study the quadrupole excited-core components of low-lying states in  $^{63}\text{Cu}$ .<sup>10,11</sup> The  $(p,t)$  reaction on an odd-proton target nucleus is a very appropriate tool for studying core excitations, since the state of the odd proton is kept unchanged to first order during this reaction process.<sup>10</sup>

While the  $(p,t)$  and inelastic scattering reactions have much in common as a means of core excitation, they provide different kinds of information, because they have essentially different reaction mechanisms. Therefore, a comparative study of the  $(p,t)$  reaction and the inelastic scattering leading to the same final nucleus may give new insights into core excitations and the particle-core-coupling in an odd-proton nucleus.

Previous experiments have studied the  $(p,p')$  or  $(p,t)$  reaction separately. For example, angular distributions of differential cross sections for the  $^{63}\text{Cu}(p,p')^{63}\text{Cu}$  reaction were previously measured at  $E_p = 17.5$  MeV (Ref. 9) and

lower energies.<sup>6,12</sup> In addition, the  $^{65}\text{Cu}(p,t)^{63}\text{Cu}$  reaction has been studied at  $E_p = 19.5$  MeV (Ref. 11) and 51.9 MeV.<sup>10</sup> However, the present paper reports a comparative study of these two reactions for the first time. The present experimental study also has better energy resolution and covers a larger range of excitation energy in  $^{63}\text{Cu}$  than the previous experiments.

### II. EXPERIMENTAL PROCEDURE

The reactions  $^{65}\text{Cu}(p,t)^{63}\text{Cu}$  and  $^{63}\text{Cu}(p,p')^{63}\text{Cu}$  have been studied at the incident proton energy of 40 MeV using the Michigan State University Isochronous Cyclotron. The particles from the target were detected by a delay-line counter<sup>13</sup> placed on the focal plane of the Enge split-pole magnetic spectrograph. Time-of-flight and energy-loss signals were used for particle selection.

#### A. $^{65}\text{Cu}(p,t)^{63}\text{Cu}$

Differential cross sections for the  $^{65}\text{Cu}(p,t)^{63}\text{Cu}$  reaction were measured over the laboratory angular range of  $6^\circ$  through  $64^\circ$ . The target was a self-supporting metallic foil of  $^{65}\text{Cu}$  with a thickness of  $250 \mu\text{g}/\text{cm}^2$ . The overall energy resolution was 16 keV. Figure 1 shows a typical spectrum. There is practically no background.

#### B. $^{63}\text{Cu}(p,p')^{63}\text{Cu}$

Differential cross sections for the proton inelastic scattering by  $^{63}\text{Cu}$  were measured over the laboratory angular range of  $8^\circ$  through  $95^\circ$ . The target was a self-supporting metallic foil of  $^{63}\text{Cu}$  with a thickness of  $520 \mu\text{g}/\text{cm}^2$ . The overall

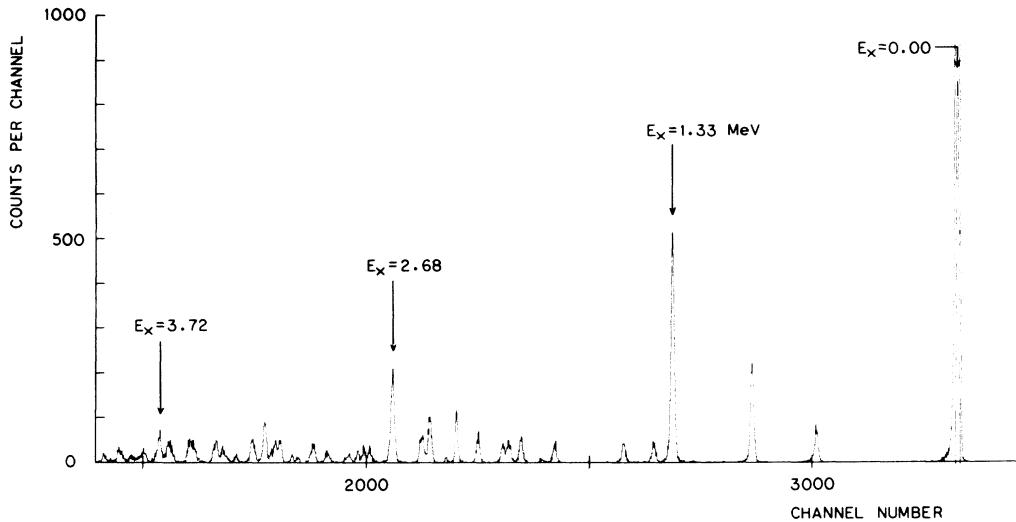


FIG. 1. Triton momentum spectrum for the reaction  $^{63}\text{Cu}(p, t)^{63}\text{Cu}$  at  $15^\circ$  lab. The excitation energy in  $^{63}\text{Cu}$  is denoted by  $E_x$ .

energy resolution was about 20 keV. Figure 2 shows a typical spectrum. The protons elastically scattered by  $^{63}\text{Cu}$  were always placed beyond the end of the delay-line counter by choosing an appropriate magnetic-field strength. This made it feasible to measure inelastic-scattering cross sections at forward angles with reasonable accuracy.

### III. EXPERIMENTAL RESULTS

#### A. $^{65}\text{Cu}(p, t)^{63}\text{Cu}$

Angular distributions of differential cross sections were obtained for 38 transitions to states

in  $^{63}\text{Cu}$  up to an excitation energy of 3.90 MeV. They are shown in Figs. 3 through 7 grouped according to their shapes. The error bars indicate only the statistical errors. There is no uncertainty from background subtraction. The absolute cross section scales in Figs. 3 through 7 are correct to within  $\pm 15\%$ .

A summary of the observed states in  $^{63}\text{Cu}$  is given in Table I. The excitation energy ( $E_x$ ) is correct to within  $\pm 0.01$  MeV for  $E_x < 2.70$  MeV, and within  $\pm 0.02$  MeV for  $E_x > 2.70$  MeV. The states reported at  $E_x = 2.51, 3.58, 3.68, 3.79,$  and 3.90 MeV in Table I appear to be unresolved

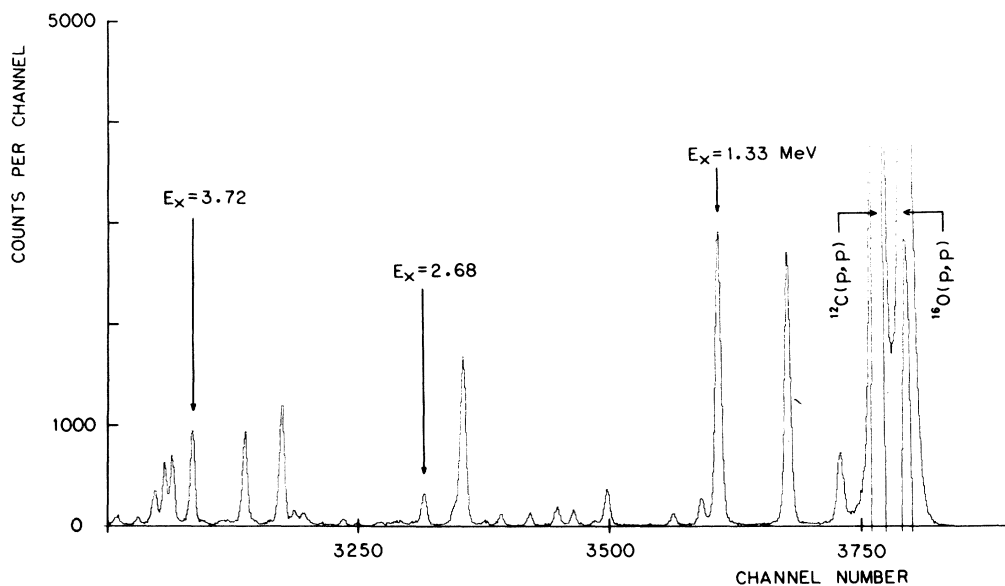


FIG. 2. Proton momentum spectrum for the reaction  $^{63}\text{Cu}(p, p')^{63}\text{Cu}$  at  $24^\circ$  lab. The excitation energy in  $^{63}\text{Cu}$  is denoted by  $E_x$ .

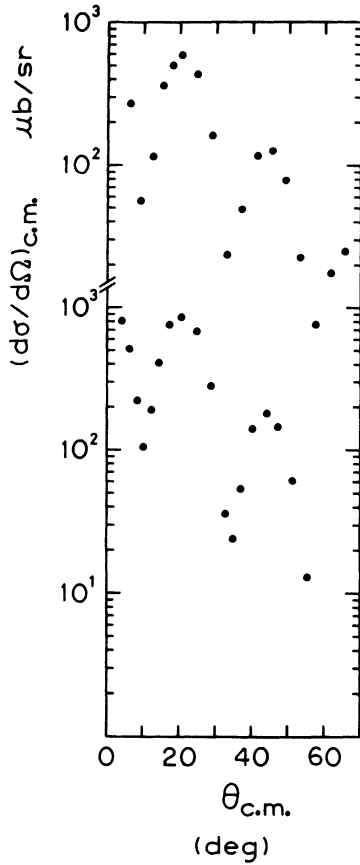


FIG. 3. The experimental angular distribution (upper) for the ground-state transition in the reaction  $^{65}\text{Cu}(p, t)^{63}\text{Cu}$ , compared with that (lower) for the ground-state transition in the "core" reaction  $^{64}\text{Ni}(p, t)^{62}\text{Ni}$  (Ref. 15).

multiplets. The possibility of unresolved multiplets is not excluded for other peaks at excitation energies higher than 3.14 MeV. The determination of the transferred angular momentum  $L$  on the basis of the angular distribution shape will be described in Sec. IV.

#### B. $^{63}\text{Cu}(p, p')^{63}\text{Cu}$

Angular distributions of differential cross sections were obtained for stronger transitions to 20 excited states up to an excitation energy of 3.89 MeV. They are shown in Figs. 8 through 11 grouped according to their shapes. In contrast to the above case of the  $(p, t)$  reaction, errors in differential cross sections originate from uncertainties in subtraction of the background and occasionally in separation of peaks. The error bars in Figs. 8 through 11 include errors of this kind. In general, the statistical errors are negligibly small. The absolute cross section scales are correct within  $\pm 15\%$ . There seem to be a

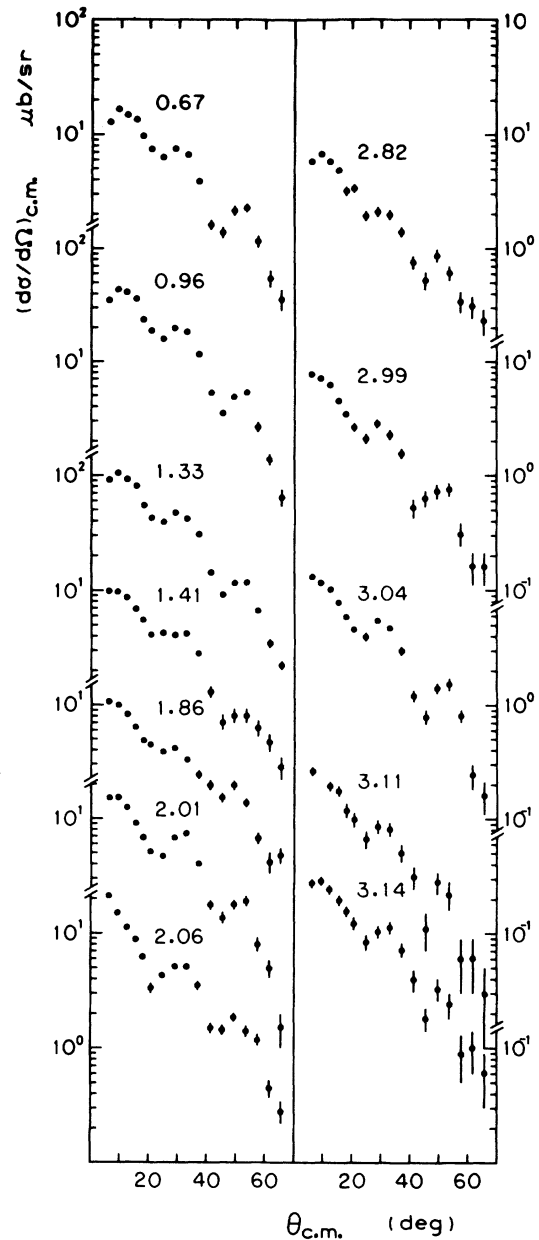


FIG. 4.  $L=2$  angular distributions in the reaction  $^{65}\text{Cu}(p, t)^{63}\text{Cu}$ . The numerical value given near each angular distribution shows the excitation energy  $E_x$  of the final state in  $^{63}\text{Cu}$  in units of MeV. The same is true for all the following figures. The angular distribution for the 1.86 MeV state is an exception, being  $L=2+4$ , and is shown here for illustrative comparison.

large number of weakly excited states at excitation energies higher than 2.68 MeV (Fig. 2). A higher energy resolution would be required to resolve individual levels.

A summary of the observed states is given in

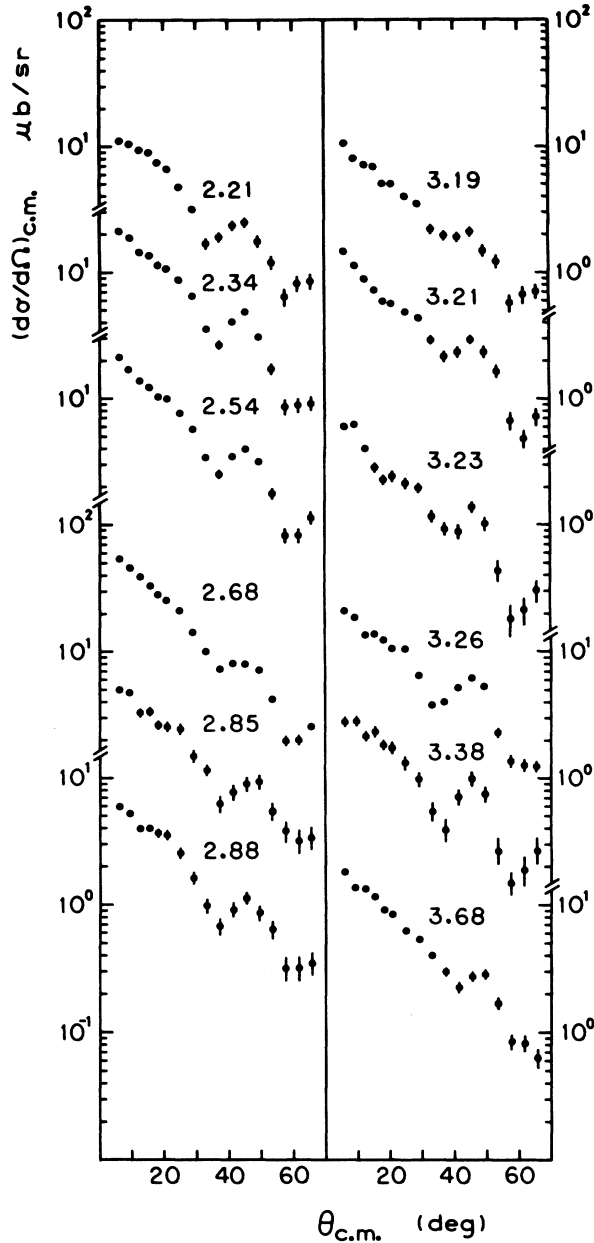


FIG. 5.  $L=4$  angular distributions in the reaction  $^{65}\text{Cu}(p, t)^{63}\text{Cu}$ . The numerical value near each angular distribution shows  $E_x$  in MeV.

Table I. The excitation energy  $E_x$  is correct within  $\pm 0.01$  MeV for  $E_x < 2.70$  MeV, and within  $\pm 0.02$  MeV for  $E_x > 2.70$  MeV. The determination of the transferred angular momentum  $L$  for each transition on the basis of the angular distribution shape will be described in Sec. IV.

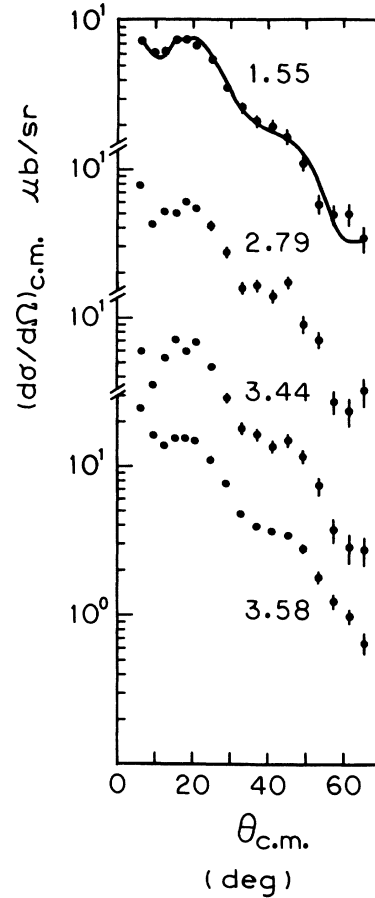


FIG. 6.  $L=0+2$  angular distributions in the reaction  $^{65}\text{Cu}(p, t)^{63}\text{Cu}$ . The solid curve shows the result of superposing the experimental angular distribution for the ground-state transition  $^{65}\text{Cu}(p, t_0)^{63}\text{Cu}$  (Fig. 3) with that for the transition to the 1.33 MeV state (Fig. 4) with a relative weight of 0.17 to 1.00.

#### IV. DETERMINATION OF THE TRANSFERRED ANGULAR MOMENTUM $L$

##### A. $^{65}\text{Cu}(p, t)^{63}\text{Cu}$

##### 1. Empirical systematics

In the  $(p, t)$  or  $(t, p)$  reaction process, only neutrons are rearranged according to the usual single-step DWBA (distorted-wave Born approximation) theory, taking account of only leading-order transition matrix elements. Thus, the  $(p, t)$  or  $(t, p)$  reaction on an odd-proton nucleus proceeds through single-step core excitations leaving the odd proton intact as a spectator.<sup>10,14</sup> By means of the experimental information on the  $(p, t)$  angular distributions for  $L=0, 2, 3,$  and  $4$  transitions obtained by a study of the "core" reaction  $^{64}\text{Ni}(p, t)^{62}\text{Ni}$  at the same incident energy of 40

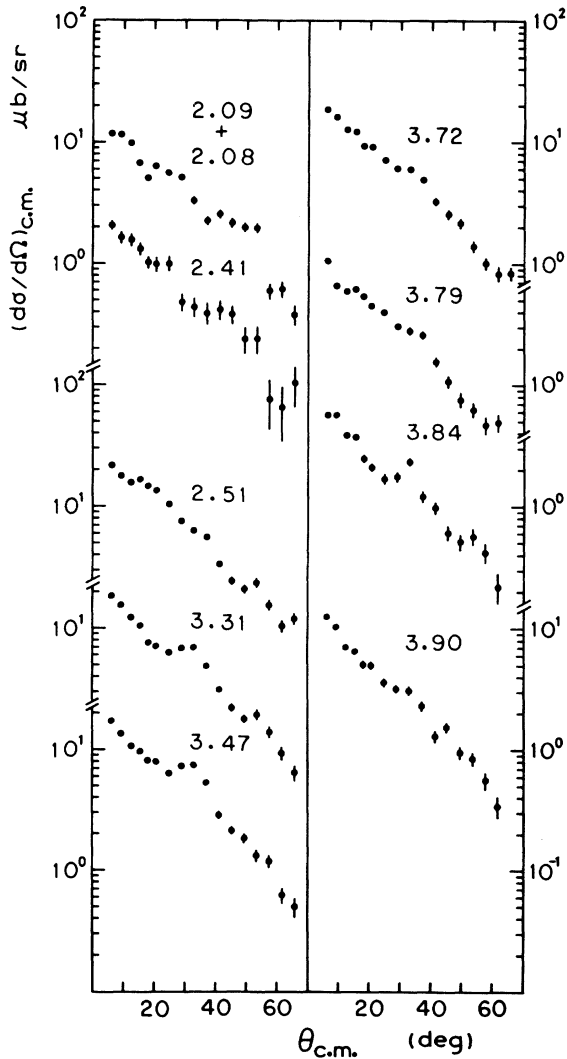


FIG. 7. Other angular distributions in the reaction  $^{65}\text{Cu}(p,t)^{63}\text{Cu}$ .

MeV,<sup>15</sup> empirical assignment of the angular-momentum transfer  $L$  was made to each transition.

Figure 3 shows the experimental angular distribution for the  $^{65}\text{Cu}(p,t)^{63}\text{Cu}$  transition to the ground state of  $^{63}\text{Cu}$  compared with that for the "core" transition  $^{64}\text{Ni}(p,t_0)^{63}\text{Ni}$ .<sup>15</sup> The two angular distributions are almost identical. Therefore, the  $^{65}\text{Cu}(p,t_0)^{63}\text{Cu}$  transition is concluded to be a rather pure  $L=0$  transition.

All the angular distributions in Fig. 4 have peaks around  $30^\circ$  and  $50^\circ$  c.m. The characteristic feature of the  $L=2$  angular distributions for the transitions to the three lowest excited states ( $E_x=0.67$ ,  $0.96$ , and  $1.33$  MeV) is the occurrence of peaks at  $10^\circ$ ,  $31^\circ$ , and  $52^\circ$  c.m. with well-defined minima in between, and this feature is possessed, too,

by the angular distribution for the transition to the 2.01 MeV state.

The angular distribution for the 1.86 MeV state indicates the presence of substantial  $L=4$  contributions filling in the valleys of the characteristic  $L=2$  angular distribution (see below). Therefore, the transition to the 1.86 MeV state is assigned to be an  $L=2+4$  transition. All the other angular distributions in Fig. 4 are assigned to be  $L=2$ .

Figure 5 shows  $L=4$  angular distributions. The angular distribution for  $E_x=3.68$  MeV, however, corresponds to an unresolved multiplet, and may have contributions of other values of  $L$ .

Figure 6 shows angular distributions for mixed  $L=0+2$  transitions. The general shapes of these angular distributions can be reproduced by superposition of the pure  $L=0$  and  $L=2$  angular distributions [for the ground-state transition  $^{65}\text{Cu}(p,t_0)^{63}\text{Cu}$  in Fig. 3 and for the transition to the 1.33 MeV state, for example, in Fig. 4]. Transition amplitudes with different values of  $L$  contribute incoherently to differential cross sections in both the  $(p,t)$  and  $(p,p')$  reactions as long as the assumption of a single-step core excitation is correct.<sup>16</sup> An example of such an angular distribution made by superposition is shown in Fig. 6 by a solid line.

Since a  $(p,t)$  transition with  $L=0$  is possible only if the final state of the residual nucleus  $^{63}\text{Cu}$  has the same spin-parity  $\frac{3}{2}^-$  as the initial ground state of  $^{65}\text{Cu}$ , observation of the presence of the  $L=0$  component in the experimental angular distribution leads directly to the assignment of  $J^\pi = \frac{3}{2}^-$  to the states at  $E_x=1.55$ ,  $2.79$ ,  $3.44$ , and  $3.58$  MeV in  $^{63}\text{Cu}$ . As the 3.58 MeV state appears to be an unresolved multiplet as already stated in Sec. III, a more accurate statement would be that there exists a  $\frac{3}{2}^-$  state near  $E_x=3.58$  MeV. The assignment of  $J^\pi = \frac{3}{2}^-$  to the 1.55 MeV state was made first by Markham and Fulbright on the basis of the  $(p,t)$  angular distribution shape at  $E_p=19.5$  MeV.<sup>11</sup> This assignment was confirmed later by studies of electromagnetic transitions<sup>17,18</sup> and is also consistent with the present  $(p,t)$  work.

Figure 7 shows other angular distributions having less characteristic shapes. The states at  $E_x=2.08$  and  $2.09$  MeV were not resolved, but the 2.09 MeV state seems to be excited more strongly than the 2.08 MeV state. The angular distribution of the summed differential cross sections for these states (Fig. 7) is assigned to have an  $L=2+4$  shape. A comparison with Figs. 4 and 5 shows that the valley around  $45^\circ$  c.m. of the  $L=2$  angular distribution is filled in by the peak of the  $L=4$  angular distribution located just at the same angular position, and that there still

TABLE I. States in  $^{63}\text{Cu}$  observed in the reactions  $^{65}\text{Cu}(\phi, t)^{63}\text{Cu}$  and  $^{63}\text{Cu}(\phi, p')^{63}\text{Cu}$ .

| $E_x$<br>(MeV)    | $^{65}\text{Cu}(\phi, t)^{63}\text{Cu}$ |                                                          | $^{63}\text{Cu}(\phi, p')^{63}\text{Cu}$ |     |                                                        | $\gamma$ -ray work <sup>a</sup>              |                                                                                  |
|-------------------|-----------------------------------------|----------------------------------------------------------|------------------------------------------|-----|--------------------------------------------------------|----------------------------------------------|----------------------------------------------------------------------------------|
|                   | $L$                                     | $(d\sigma/d\Omega)_{\text{max}}$<br>( $\mu\text{b/sr}$ ) | $E_x$<br>(MeV)                           | $L$ | $(d\sigma/d\Omega)_{\text{max}}$<br>( $\text{mb/sr}$ ) | $E_x$<br>(MeV)                               | $J^\pi$                                                                          |
| 0.00              | 0                                       | 588                                                      |                                          |     |                                                        | 0.0000                                       | $\frac{3}{2}^-$                                                                  |
| 0.67              | 2                                       | 16.4                                                     | 0.67                                     | 2   | 2.27                                                   | 0.6696                                       | $\frac{1}{2}^-$                                                                  |
| 0.96              | 2                                       | 43.5                                                     | 0.96                                     | 2   | 9.41                                                   | 0.9621                                       | $\frac{5}{2}^-$                                                                  |
| 1.33              | 2                                       | 103                                                      | 1.33                                     | 2   | 9.47                                                   | 1.3270                                       | $\frac{7}{2}^-$                                                                  |
| 1.41              | 2                                       | 9.9                                                      | 1.41                                     | 2   | 0.95                                                   | 1.4120                                       | $\frac{5}{2}^-$                                                                  |
| 1.55              | 0+2                                     | 7.4                                                      | 1.55                                     | 2   | 0.60                                                   | 1.5470                                       | $\frac{3}{2}^-$                                                                  |
| 1.86              | 2+4                                     | 10.8                                                     | 1.86                                     | 2+4 | 0.69                                                   | 1.8612                                       | $\frac{7}{2}^-$                                                                  |
| 2.01              | 2                                       | 15.2                                                     | 2.01                                     | 2   | 0.34                                                   | 2.0112                                       | $\frac{3}{2}^-$                                                                  |
| 2.06              | 2                                       | 15.1                                                     |                                          |     |                                                        | 2.0622                                       | $\frac{1}{2}^-, \frac{3}{2}^-$                                                   |
| 2.08              | 2+4                                     | 11.7                                                     | 2.08                                     | 2+4 | 0.25                                                   | 2.0815                                       | $\frac{5}{2}^-$                                                                  |
| 2.09              |                                         |                                                          |                                          |     |                                                        |                                              | 2.0927                                                                           |
| 2.21              | 4                                       | 11.0                                                     | 2.21                                     | 4   | 0.21                                                   | 2.2080                                       | $\frac{9}{2}^-$                                                                  |
| 2.34              | 4                                       | 21.0                                                     | 2.34                                     | 4   | 0.10                                                   | 2.3365                                       | $\frac{5}{2}^-$                                                                  |
| 2.41              | 2+4                                     | 2.1                                                      | 2.41                                     | 2+4 | 0.13                                                   | 2.4048                                       | $\frac{7}{2}^-$                                                                  |
| 2.51 <sup>b</sup> | (0+2)+3                                 | 21.6                                                     | 2.51                                     | 3   | 1.83                                                   | { 2.4971 <sup>c</sup><br>2.5120 <sup>c</sup> | $\frac{3}{2}^- (\frac{5}{2}^-)$<br>$\frac{1}{2}^-, \frac{3}{2}^-, \frac{5}{2}^-$ |
| 2.54              | 4                                       | 21.4                                                     | 2.54                                     | 4   | 0.27                                                   | 2.5358 <sup>d</sup>                          | $\frac{5}{2}^-$                                                                  |
| 2.68              | 4                                       | 53.8                                                     | 2.68                                     | 4   | 0.55                                                   |                                              |                                                                                  |
| 2.79              | 0+2                                     | 6.0                                                      |                                          |     |                                                        |                                              |                                                                                  |
| 2.82              | 2                                       | 6.5                                                      |                                          |     |                                                        |                                              |                                                                                  |
| 2.85              | 4                                       | 5.0                                                      |                                          |     |                                                        |                                              |                                                                                  |
| 2.88              | 4                                       | 6.0                                                      |                                          |     |                                                        |                                              |                                                                                  |
| 2.99              | 2                                       | 7.1                                                      |                                          |     |                                                        |                                              |                                                                                  |
| 3.04              | 2                                       | 11.6                                                     |                                          |     |                                                        |                                              |                                                                                  |
| 3.11              | 2                                       | 2.6                                                      |                                          |     |                                                        |                                              |                                                                                  |
| 3.14              | 2                                       | 2.9                                                      |                                          |     |                                                        |                                              |                                                                                  |
| 3.19              | 4                                       | 10.6                                                     |                                          |     |                                                        |                                              |                                                                                  |
| 3.21              | 4                                       | 14.7                                                     |                                          |     |                                                        |                                              |                                                                                  |
| 3.23              | 4                                       | 6.2                                                      |                                          |     |                                                        |                                              |                                                                                  |
| 3.26              | 4                                       | 21.0                                                     |                                          |     |                                                        |                                              |                                                                                  |
| 3.31              | (?)+3                                   | 18.5                                                     | 3.32                                     | 3   | 1.12                                                   |                                              |                                                                                  |
| 3.38              | 4                                       | 2.8                                                      |                                          |     |                                                        |                                              |                                                                                  |
| 3.44              | 0+2                                     | 7.0                                                      |                                          |     |                                                        |                                              |                                                                                  |
| 3.47              | (?)+3                                   | 17.3                                                     | 3.48                                     | 3   | 0.86                                                   |                                              |                                                                                  |
| 3.58 <sup>b</sup> | 0+2                                     | 15.4                                                     |                                          |     |                                                        |                                              |                                                                                  |
| 3.68 <sup>b</sup> | 4+(?)                                   | 18.0                                                     |                                          |     |                                                        |                                              |                                                                                  |
| 3.72              | (?)+3                                   | 18.5                                                     | 3.72                                     | 3   | 0.81                                                   |                                              |                                                                                  |
| 3.79 <sup>b</sup> | (?)+3                                   | 10.4                                                     | 3.81                                     | 3   | 0.60                                                   |                                              |                                                                                  |
| 3.84              | (?)+3                                   | 5.7                                                      | 3.84                                     | 3   | 0.52                                                   |                                              |                                                                                  |
| 3.90 <sup>b</sup> | (?)+3                                   | 12.6                                                     | 3.89                                     | 3   | 0.34                                                   |                                              |                                                                                  |

<sup>a</sup> Reference 18.<sup>c</sup> See text (Sec. IV A 1).<sup>b</sup> Unresolved multiplet.<sup>d</sup> See text (Sec. VI B 3).

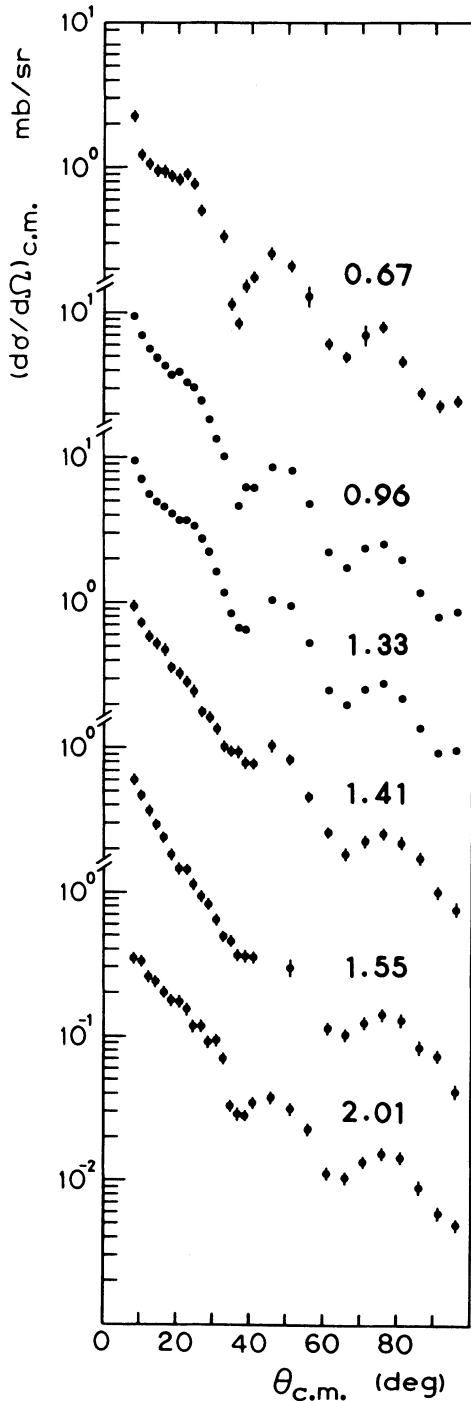


FIG. 8.  $L=2$  angular distributions in the reaction  $^{63}\text{Cu}(p, p')^{63}\text{Cu}$ .

remain traces of the characteristic peaks of the  $L=2$  angular distribution around  $10^\circ$ ,  $30^\circ$ , and  $50^\circ$ . The angular distribution for the 2.41 MeV state seems to have qualitatively the same features as the above one, but with a dominant con-

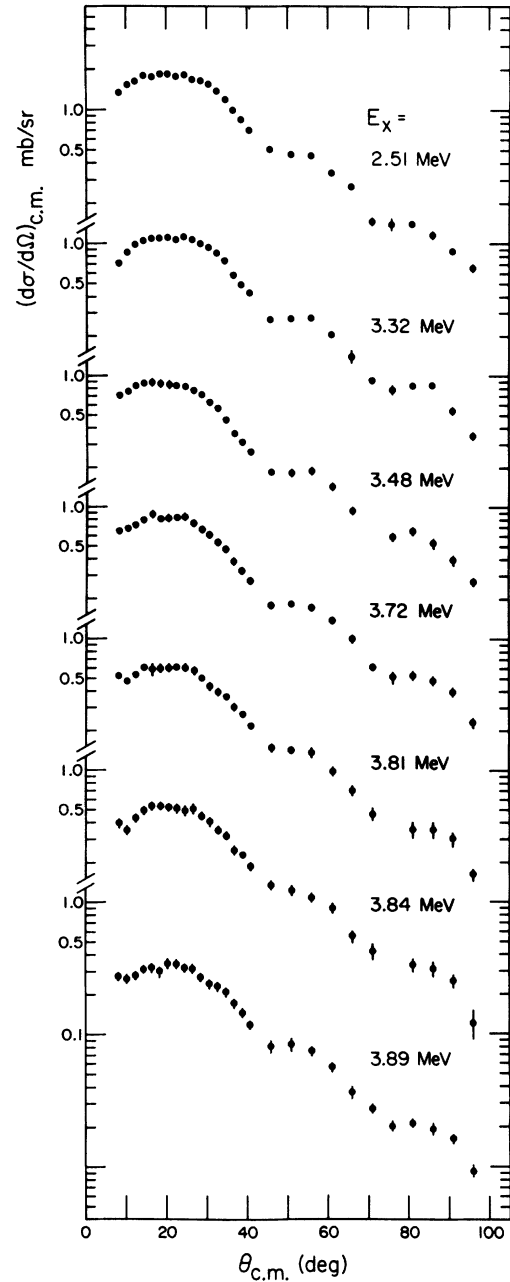


FIG. 9.  $L=3$  angular distributions in the reaction  $^{63}\text{Cu}(p, p')^{63}\text{Cu}$ .

tribution of  $L=4$ .

There are at least three states reported at excitation energies very near 2.51 MeV. Recent gamma-ray work reported a state at  $E_x = 2.4971$  MeV with  $J^\pi = \frac{3}{2}^-$  or  $\frac{5}{2}^-$  and another one at  $E_x = 2.5120$  MeV with  $J^\pi = \frac{1}{2}^-$ ,  $\frac{3}{2}^-$ , or  $\frac{5}{2}^-$ .<sup>18</sup> On the other hand,  $^{62}\text{Ni}(^3\text{He}, d)^{63}\text{Cu}$  data showed the existence of a state with  $J^\pi = \frac{3}{2}^+$  at  $E_x = 2.51$  MeV

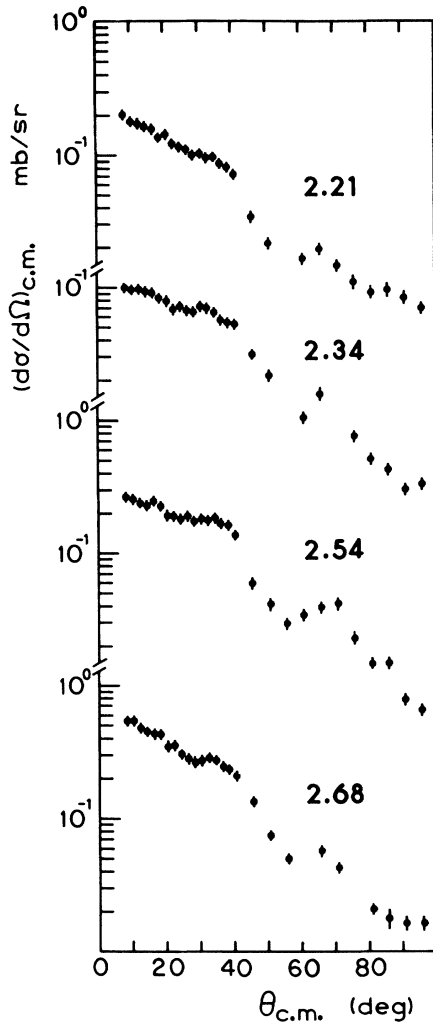


FIG. 10.  $L=4$  angular distributions in the reaction  $^{63}\text{Cu}(p, p')^{63}\text{Cu}$ .

(Ref. 19) or  $E_x = 2.500$  MeV.<sup>20</sup> With the energy resolution (0.016 MeV) and the accuracy in  $E_x$  ( $\pm 0.01$  MeV) of the present experiment, it is impossible to uniquely identify the peak observed in the present experiment at  $E_x = 2.51$  MeV with any one of the three previously reported states. The  $(p, t)$  work of Markham and Fulbright at  $E_p = 19.5$  MeV reported a state at  $E_x = 2.498$  MeV,<sup>11</sup> which may be identified with the 2.4971 MeV state observed in the gamma-ray work.<sup>18</sup> They assign  $J^\pi = \frac{3}{2}^-$  to this state based on the fact that the shape of the angular distribution is that of an  $L=0+2$  transition.<sup>11</sup> Referring to the  $(p, t)$  angular distribution for the 2.51 MeV state in Fig. 7, the part that lies in the angular range more forward than  $30^\circ$  c.m. also suggests an  $L=0+2$  transition. The overall shape of the angular distribution cannot be reproduced, however, by superposition

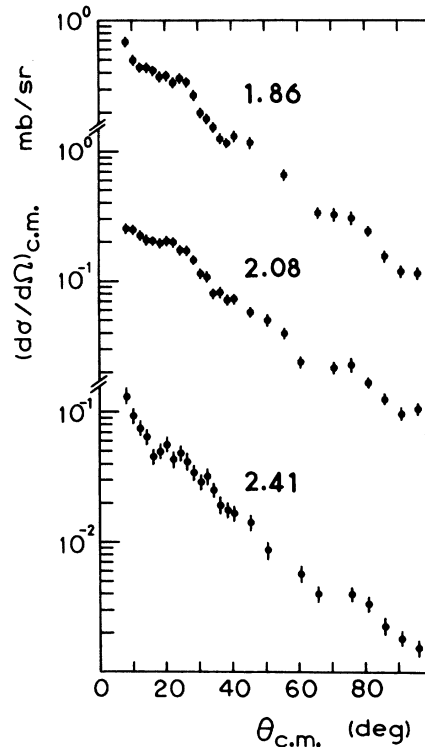


FIG. 11. Other angular distributions in the reaction  $^{63}\text{Cu}(p, p')^{63}\text{Cu}$ .

of the  $L=0$  and  $L=2$  angular distributions. In contrast to the  $L=0+2$  angular distributions in Fig. 6, the angular distribution for the 2.51 MeV state in Fig. 7 has a small hump instead of a dip in the angular range from  $30^\circ$  to  $40^\circ$  c.m., and a dip instead of a hump in the angular range of  $40^\circ$  through  $54^\circ$  c.m. These features indicate an admixture of the  $L=3$  contribution corresponding to the excitation of the above mentioned  $\frac{3}{2}^+$  state found by the  $(^3\text{He}, d)$  reaction, since the pure  $L=3$  angular distribution has a peak in the angular range of about  $30^\circ$  through  $40^\circ$  c.m. followed by a sharp fall around  $50^\circ$  c.m.<sup>15</sup> Thus, the experimental angular distribution for  $E_x = 2.51$  MeV in Fig. 7 apparently corresponds to summed differential cross sections for at least two final states.

A rise is observed in the angular range of about  $30^\circ$  through  $40^\circ$  c.m. on all the angular distributions for the transitions to the states at  $E_x = 3.31, 3.47, 3.72, 3.79, 3.84,$  and  $3.90$  MeV, in addition to the one for the transition to the 2.51 MeV. This indicates the occurrence of an  $L=3$  contribution.<sup>15</sup> It is not feasible, however, to pin down the magnitudes of the  $L=3$  contributions in the angular distributions, nor to determine what other values of  $L$  contribute to them. The 3.79 and 3.90 MeV states are unresolved multiplets.



## 2. DWBA calculation

The empirical  $L$  assignments made above are corroborated by DWBA calculations using the zero-range DWBA code DWUCK 72.<sup>21</sup> Figure 12 shows calculated angular distributions for  $L=0, 2, 3,$  and  $4$  together with typical experimental angular distributions for  $L=0, 2,$  and  $4$ . It is seen that there is no ambiguity in distinguishing between pure  $L=0, 2, 3,$  and  $4$  angular distributions. The potentials used in the calculations are given in Table II. The proton optical potential is the standard Becchetti-Greenlees potential.<sup>22</sup> The stability of the calculated DWBA curves was tested by varying each one of the tritium optical parameters. The overall shape of the calculated angular distribution is stable to the extent that no misassignment of  $L$  can occur for a pure  $L=0, 2, 3,$  or  $4$  transition.

B.  $^{63}\text{Cu}(p, p')^{63}\text{Cu}$ 

## 1. Empirical systematics

About a decade ago, a number of  $(p, p')$  experiments were performed on even-even medium-mass nuclei at incident energies of about 40 MeV.<sup>23, 24</sup> Empirical  $(p, p')$  angular distributions for  $L=2, 3,$  and  $4$  are well established. By means of these empirical systematics,  $L$  assignment was made to each  $(p, p')$  transition on the basis of the experimental angular distribution shape. The angular distributions for stronger  $L=2, 3,$  and  $4$  transitions observed in the present experiment agree with the  $L=2, 3,$  and  $4$  angular distributions observed in a previous  $(p, p')$  experiment on the core nucleus  $^{62}\text{Ni}$  at the same energy of 40 MeV,<sup>24</sup> within the experimental errors of the latter experiment.

Figure 8 shows  $L=2$  angular distributions. There are peaks around  $47^\circ$  and  $76^\circ$  c.m., and a valley around  $66^\circ$  c.m. on all of them. A bump is observed in the angular range from about  $20^\circ$  to  $32^\circ$  c.m. on the angular distributions for the 0.67, 0.96, 1.33, and 2.01 MeV states, but not on those for the 1.41 and 1.55 MeV states.

Figures 9 and 10 show  $L=3$  and  $L=4$  angular distributions. Other angular distributions are

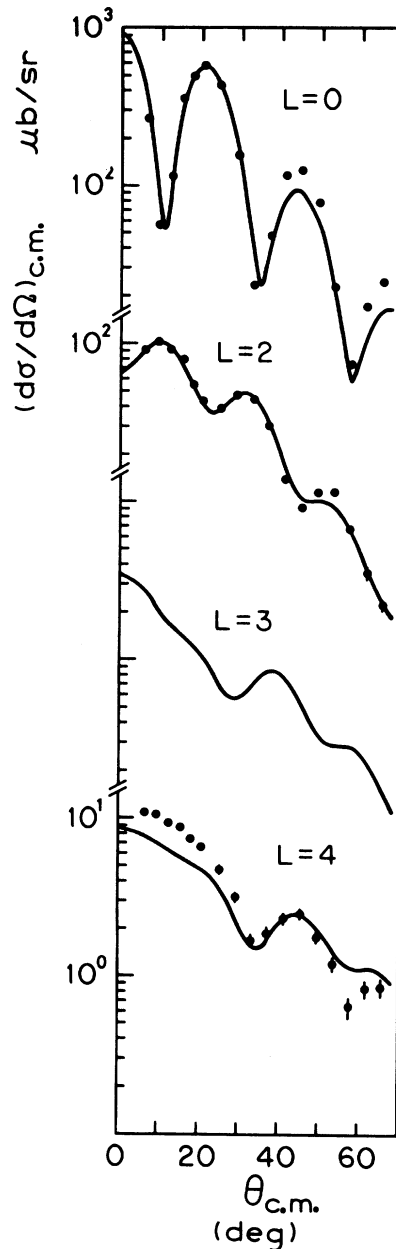


FIG. 12.  $L=0, 2, 3,$  and  $4$  angular distributions in the reaction  $^{63}\text{Cu}(p, t)^{63}\text{Cu}$  calculated by the zero-range DWBA code DWUCK 72. The experimental data are for the transitions to the ground, 1.33, and 2.21 MeV states.

TABLE II. Potential parameters used in the DWBA calculations.

|     | $V$<br>(MeV)        | $W_D$<br>(MeV) | $W$<br>(MeV) | $V_\infty$<br>(MeV) | $r_0$<br>(fm) | $r'_0$<br>(fm) | $r''_0$<br>(fm) | $r_{0\infty}$<br>(fm) | $a$<br>(fm) | $a'$<br>(fm) | $a''$<br>(fm) | $a_\infty$<br>(fm) |
|-----|---------------------|----------------|--------------|---------------------|---------------|----------------|-----------------|-----------------------|-------------|--------------|---------------|--------------------|
| $p$ | 46.67               | 3.09           | 6.10         | 6.20                | 1.17          | 1.32           | 1.32            | 1.01                  | 0.75        | 0.59         | 0.59          | 0.75               |
| $t$ | 169.7               | 0              | 22.8         | 0                   | 1.10          |                | 1.51            |                       | 0.832       |              | 0.796         |                    |
| $n$ | Varied <sup>a</sup> | 0              | 0            | Varied <sup>b</sup> | 1.25          |                |                 | 1.25                  | 0.65        |              |               | 0.65               |

<sup>a</sup> The wave function for a bound neutron is calculated by the well-depth method.

<sup>b</sup> 25 Thomas units.

shown in Fig. 11. All these angular distributions are assigned to be  $L = 2 + 4$  by a comparison with the angular distributions in Figs. 8 and 10. The bumps around  $25^\circ$  and  $76^\circ$  are traces of the  $L = 2$  contribution. The valley around  $66^\circ$  c.m. of the  $L = 2$  angular distribution is filled in by the peak of the  $L = 4$  at the same angular position, and the peak around  $47^\circ$  c.m. of the  $L = 2$  angular distribution is canceled by the sharp fall of the  $L = 4$ .

## 2. DWBA calculation

The above empirical  $L$  assignments are further corroborated by DWBA (dynamical collective model) calculations made by the zero-range DWBA code DWUCK 72.<sup>21</sup> Figure 13 shows results of DWBA calculations using the Becchetti-Greenlees proton optical potential (Table II) in comparison with experimental data. It is seen that there is no ambiguity in distinguishing between the  $L = 2, 3$ , and 4 angular distributions.

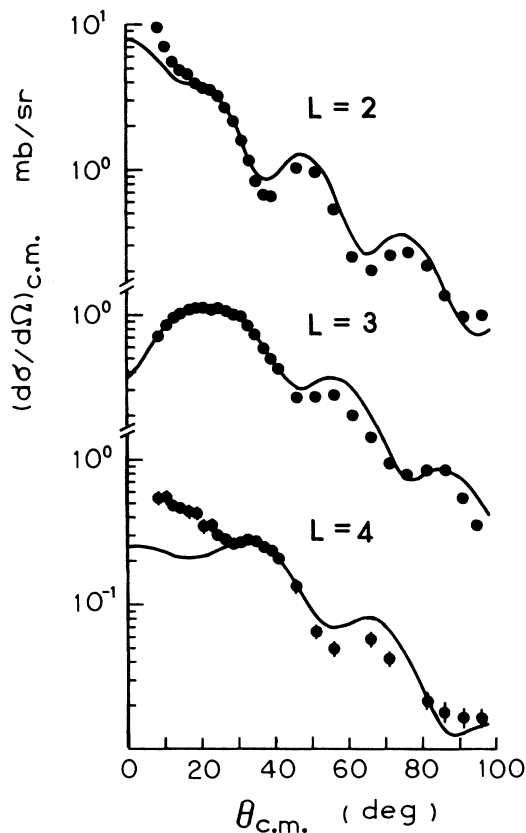


FIG. 13.  $L = 2, 3$ , and 4 angular distributions in the reaction  $^{63}\text{Cu}(p, p')^{63}\text{Cu}$  calculated by the zero-range DWBA code DWUCK 72. The experimental data are for the transitions to the 1.33, 3.32, and 2.68 MeV states.

## V. DISTRIBUTION OF THE TRANSITION STRENGTH FOR EACH MULTIPOLE $L$

### A. $L = 0$

Monopole core excitation is observed only in the  $^{65}\text{Cu}(p, t)^{63}\text{Cu}$  reaction. Only the ground-state transition is purely  $L = 0$ .

Mixed  $L = 0 + 2$  transitions are observed leading to four states at  $E_x = 1.55, 2.79, 3.44$ , and 3.58 MeV (Fig. 14). The distribution in  $E_x$  of the  $L = 0$  strength for  $^{63}\text{Cu}$  is qualitatively in agreement with that for the core nucleus  $^{62}\text{Ni}$ , as shown in Fig. 14. Seth and collaborators found for  $1f_{7/2}$ -shell nuclei that a single state in an odd nucleus carried a major fraction of the  $L = 0$  strength of the first excited  $0^+$  state in the even-even core nucleus, and that the state in the odd nucleus was located approximately 0.4 MeV lower in  $E_x$  than its counterpart in the core nucleus.<sup>25, 26</sup> The correspondence between the 1.55 MeV state in  $^{63}\text{Cu}$  and the 2.05 MeV state in  $^{62}\text{Ni}$  (Fig. 14) indicates that the systematic behavior found by Seth *et al.* persists beyond the  $1f_{7/2}$ -shell closure. However, the 1.55 MeV state is of a complex nature, as is suggested by the large  $L = 2$  contribution in its excitation (Fig. 6), and will be discussed in detail in Sec. VI.

### B. $L = 2$

The distribution in  $E_x$  of the  $L = 2$  transition strength is shown in Fig. 14. Six  $L = 2$  transitions are observed in the  $^{63}\text{Cu}(p, p')^{63}\text{Cu}$  reaction leading to states at  $E_x = 0.67, 0.96, 1.33, 1.41, 1.55$ , and 2.01 MeV. All these states are excited also in the  $^{65}\text{Cu}(p, t)^{63}\text{Cu}$  reaction. The state at  $E_x = 2.06$  MeV observed in the  $^{65}\text{Cu}(p, t)^{63}\text{Cu}$  is missing in the  $^{63}\text{Cu}(p, p')^{63}\text{Cu}$ . The  $(p, t)$  transition to the 1.55 MeV state has also a large  $L = 0$  contribution (see above).

### C. $L = 3$

Information on the  $L = 3$  transition strength was obtained only from the  $^{63}\text{Cu}(p, p')^{63}\text{Cu}$ , and is shown in Fig. 15. The octupole transitions have been already reported and discussed in a separate paper.<sup>27</sup>

As expected, the octupole core excitation is weak in the  $^{65}\text{Cu}(p, t)^{63}\text{Cu}$  reaction. The collective octupole excitation is made up of a coherent superposition of particle-hole excitations that lift a nucleon to the next major shell,<sup>28</sup> whereas the  $(p, t)$  reaction has large amplitudes only for production of two holes (hole-hole excitations) in the same major shell.

### D. $L = 4$

The distribution in  $E_x$  of the  $L = 4$  transition strength is shown in Fig. 16. In both the

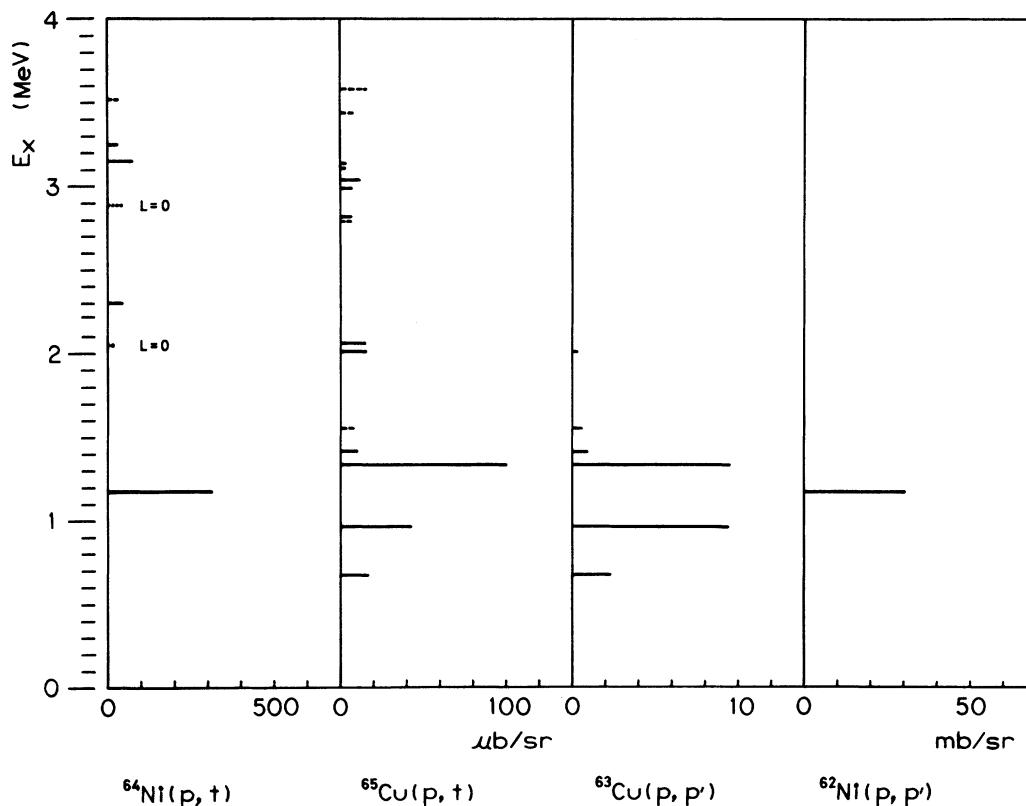


FIG. 14. Distributions of the  $L=0$  and  $L=2$  transition strengths. Peak cross sections in the reactions  $^{64}\text{Ni}(p,t)^{62}\text{Ni}$  (Ref. 15),  $^{65}\text{Cu}(p,t)^{63}\text{Cu}$ ,  $^{63}\text{Cu}(p,p')^{63}\text{Cu}$ , and  $^{62}\text{Ni}(p,p')^{62}\text{Ni}$  (Ref. 24) are shown. Dotted segments signify pure  $L=0$  transitions, and dashed segments mixed  $L=0+2$  ones. Solid segments signify  $L=2$  transitions.

$^{65}\text{Cu}(p,t)^{63}\text{Cu}$  and  $^{63}\text{Cu}(p,p')^{63}\text{Cu}$  reactions, a quartet of  $L=4$  transitions is observed leading to states at  $E_x=2.21, 2.34, 2.54,$  and  $2.68$  MeV. These  $L=4$  assignments have been made for the first time, except for the  $(p,t)$  transition to the 2.54 MeV state which was assigned to be  $L=4$  by a previous  $(p,t)$  experiment at  $E_p=19.5$  MeV.<sup>11</sup> There are also two states at  $E_x=2.85$  and  $2.88$  MeV excited by weak  $L=4$  transitions in the  $^{65}\text{Cu}(p,t)^{63}\text{Cu}$  reaction. Small peaks are observed at  $E_x=2.85$  and  $2.88$  MeV in  $^{63}\text{Cu}(p,p')^{63}\text{Cu}$  spectra. Differential cross sections, however, were not derived for these peaks because of very large uncertainties in background subtraction. Still higher in  $E_x$ , the  $(p,t)$  data show the existence of another  $L=4$  quartet with very closely spaced members at  $E_x=3.19, 3.21, 3.23,$  and  $3.26$  MeV.

## VI. DISCUSSION

### A. General remarks on the core excitation in the reactions $^{65}\text{Cu}(p,t)^{63}\text{Cu}$ and $^{63}\text{Cu}(p,p')^{63}\text{Cu}$

Comprehensive theoretical study of the structure of  $^{63}\text{Cu}$  has so far been limited to low-lying states

( $E_x < 2.01$  MeV).<sup>2,4,5,11,29</sup> In the simplest excited-core model for  $^{63}\text{Cu}$ , the ground state of  $^{63}\text{Cu}$  is the pure proton single-particle state  $[2p_{3/2} \otimes 0_1^+(\text{core})]_{3/2}$  with the odd proton occupying the  $2p_{3/2}$  orbital coupled with the ground state of the core nucleus  $^{62}\text{Ni}$ . There arises a quartet of excited states  $[2p_{3/2} \otimes 2_1^+]_{1/2,3/2,5/2,7/2}$  by the coupling of the  $2p_{3/2}$  proton orbital with the first excited state of the core.<sup>5-8</sup> The inadequacy of this model was recognized quite early in both experimental and theoretical studies.<sup>2,9</sup> Deviations from the model are produced by particle-core interactions with a rather strong quadrupole-quadrupole part and the occurrence of the proton single-particle states  $[2p_{1/2} \otimes 0_1^+]_{1/2}$  and  $[1f_{5/2} \otimes 0_1^+]_{5/2}$  in addition to the  $[2p_{3/2} \otimes 0_1^+]_{3/2}$ . The particle-core interactions mix the excited-core states and single-particle states.<sup>2,5,30</sup> In particular, the ground state is now a linear combination of components such as  $[2p_{3/2} \otimes 0_1^+]_{3/2}$ ,  $[2p_{3/2} \otimes 2_1^+]_{3/2}$ ,  $[2p_{1/2} \otimes 2_1^+]_{3/2}$ ,  $[1f_{5/2} \otimes 2_1^+]_{3/2}$ , etc.<sup>2,30</sup> Even if the reaction mechanism of the proton inelastic scattering is a single-step core excitation leaving the

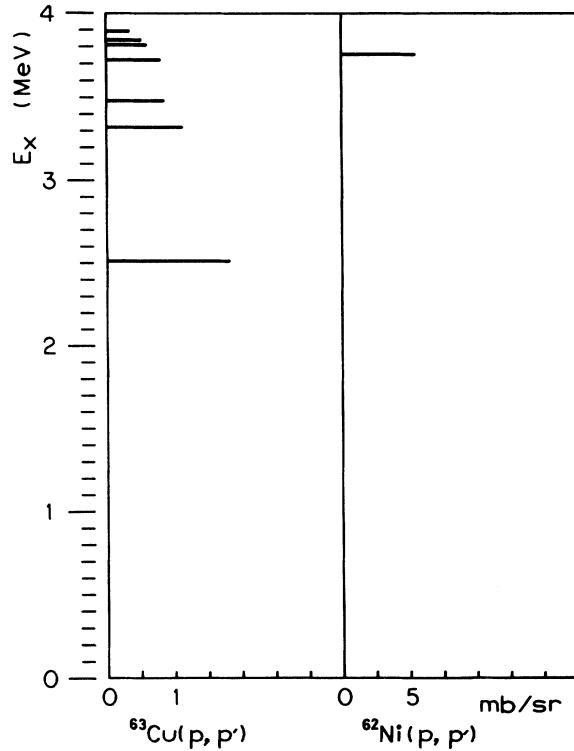


FIG. 15. Distribution of the  $L = 3$  transition strength. Peak cross sections in the reactions  $^{63}\text{Cu}(p, p')^{63}\text{Cu}$  and  $^{62}\text{Ni}(p, p')^{62}\text{Ni}$  are shown.

odd proton intact as a spectator, the occurrence of excited-core configurations in the ground state makes the physical picture far from the simple weak-coupling excited-core model. For example, the following three reduced matrix elements are involved in the  $(p, p')$  core excitation of the low-lying states, provided no other collective states of the core other than the  $2_1^+$  are mixed into the ground state of  $^{63}\text{Cu}$  (if other collective states are present, too, the number of reduced matrix elements is larger):

$$\langle 62; 2_1^+ || \hat{Y}_2 || 0_1^+; 62 \rangle, \quad (1)$$

$$\langle 62; 2_1^+ || \hat{Y}_2 || 2_1^+; 62 \rangle, \quad (2)$$

and

$$\langle 62; 0_1^+ || \hat{Y}_2 || 2_1^+; 62 \rangle \quad (3)$$

$$(\equiv \langle 62; 2_1^+ || \hat{Y}_2 || 0_1^+; 62 \rangle^*),$$

where  $\hat{Y}_2$  is the quadrupole core-excitation operator due to the nuclear interactions of the incident proton with the core, and 62 denotes the mass number of the core nucleus,  $^{62}\text{Ni}$ . Since the three core-excitation matrix elements contribute coherently, the relative cross sections for the low-lying states are very sensitive to the mixed wave functions and the relative values of (1), (2), and (3). In this situation, it is not pos-

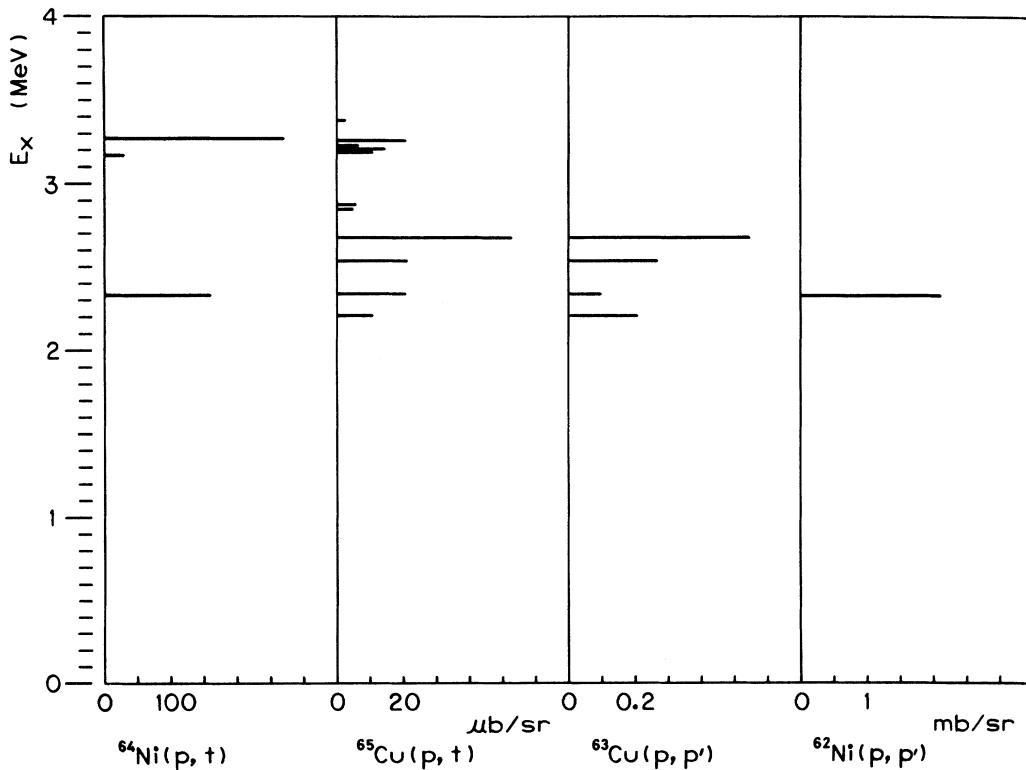


FIG. 16. Distribution of the  $L = 4$  transition strength. Peak cross sections in the reactions  $^{64}\text{Ni}(p, t)^{62}\text{Ni}$ ,  $^{65}\text{Cu}(p, t)^{63}\text{Cu}$ ,  $^{63}\text{Cu}(p, p')^{63}\text{Cu}$ , and  $^{62}\text{Ni}(p, p')^{62}\text{Ni}$  are shown.

sible to apply the  $(2J+1)$  rule<sup>6-8</sup> as well as a sum-rule argument that compares the sum of the cross sections for the excited-core states with the cross section for the corresponding core state in  $^{62}\text{Ni}$ .<sup>6-8</sup> The  $(2J+1)$  rule and a sum-rule argument make sense provided only the reduced matrix element (1) is involved in the core excitation.

The situation is similar in the  $^{65}\text{Cu}(p, t)^{63}\text{Cu}$  reaction. In the core excitation of the low-lying states in  $^{63}\text{Cu}$ , the following three reduced matrix elements contribute coherently to the cross sections:

$$\langle 62; 2_1^+ || \hat{Y}'_2 || 0_1^+; 64 \rangle, \quad (1')$$

$$\langle 62; 2_1^+ || \hat{Y}'_2 || 2_1^+; 64 \rangle, \quad (2')$$

and

$$\langle 62; 0_1^+ || \hat{Y}'_2 || 2_1^+; 64 \rangle, \quad (3')$$

where  $\hat{Y}'_2$  is the  $L=2$  two-neutron-annihilation operator, and 62 and 64 stand for the core nuclei  $^{62}\text{Ni}$  and  $^{64}\text{Ni}$ .

Within the framework of a model that assumes the single-step core excitation as the only mechanism for both the  $^{63}\text{Cu}(p, p')^{63}\text{Cu}$  and  $^{65}\text{Cu}(p, t)^{63}\text{Cu}$  reactions, the only sources of differences between the relative cross sections for the same final states in the reactions  $^{63}\text{Cu}(p, p')^{63}\text{Cu}$  and  $^{65}\text{Cu}(p, t)^{63}\text{Cu}$  are the differences between the relative values of the reduced matrix elements (1) through (3) and (1') through (3'), as well as the difference between the particle-core wave functions for the ground states of  $^{63}\text{Cu}$  and  $^{65}\text{Cu}$  in the entrance channels of the reactions. If the ground states of  $^{63}\text{Cu}$  and  $^{65}\text{Cu}$  have the same particle-core wave function, and if the relative values of the matrix elements (1) through (3) are equal to those of (1') through (3'), the relative cross sections for the low-lying states in the  $^{63}\text{Cu}(p, p')^{63}\text{Cu}$  are equal to those in the  $^{65}\text{Cu}(p, t)^{63}\text{Cu}$ . Other detailed differences between the  $(p, p')$  and  $(p, t)$  reactions are irrelevant, as far as the relative cross sections are concerned. More discussion of this point will be given in Sec. VIC and VID.

Similar statements apply to higher-lying excited-core states. For example, hexadecapole excited-core states are excited coherently by the reduced matrix elements

$$\langle 62; 4_1^+ || \hat{Y}'_4 || 0_1^+; 62 \rangle, \quad (4)$$

and

$$\langle 62; 4_1^+ || \hat{Y}'_4 || 2_1^+; 62 \rangle \quad (5)$$

in the  $^{63}\text{Cu}(p, p')^{63}\text{Cu}$ , and by

$$\langle 62; 4_1^+ || \hat{Y}'_4 || 0_1^+; 64 \rangle, \quad (4')$$

and

$$\langle 62; 4_1^+ || \hat{Y}'_4 || 2_1^+; 64 \rangle \quad (5')$$

in the  $^{65}\text{Cu}(p, t)^{63}\text{Cu}$ , where  $\hat{Y}'_4$  and  $\hat{Y}'_4'$  are the hexadecapole core-excitation operators conserving the neutron number and decreasing it by 2, respectively. Even if the weak-coupling picture is correct for the hexadecapole excited-core states, the  $(2J+1)$  rule and a sum-rule argument are not applicable to them in general because of the occurrence of a transition amplitude involving the matrix element (5) or (5') in addition to the one involving (4) or (4'). In other words, deviations from the  $(2J+1)$  rule or a sum rule do not necessarily mean breakdown of the weak-coupling picture for the hexadecapole states. Although the low-lying quadrupole excited-core states are subjected to a substantial particle-core mixing, there still remains a possibility that the weak-coupling picture may be applicable to the octupole and quadrupole excited-core states. No comprehensive theoretical study has been done for the octupole and hexadecapole states in  $^{63}\text{Cu}$ .

## B. Grouping of excited states in $^{63}\text{Cu}$ into excited-core multiplets

### 1. Quadrupole multiplets

Although the low-lying excited states in  $^{63}\text{Cu}$  were interpreted at first by the simple excited-core model,<sup>6-8</sup> the existence of relatively closely spaced proton single-particle orbitals  $2p_{3/2}$ ,  $2p_{1/2}$ , and  $1f_{5/2}$  and the substantial quadrupole-quadrupole particle-core interactions complicate the situation. Even the large volume of the theoretical literature testifies to the importance and the difficulty of the subject.<sup>2, 4, 5, 29, 30</sup>

In the early days, the greatest puzzle on the experimental side was the missing  $[2p_{3/2} \otimes 2_1^+]_{3/2}$  state. Markham and Fulbright assigned  $J^\pi = \frac{3}{2}^-$  to a state at  $E_x = 1.547$  MeV and identified it with the configuration  $[2p_{3/2} \otimes 2_1^+]_{3/2}$ , as no other states were established to have  $J^\pi = \frac{3}{2}^-$  at that time.<sup>11</sup> De Jager and Boeker performed calculations assuming the 1.55 MeV state to be the  $[2p_{3/2} \otimes 2_1^+]_{3/2}$ , but further considered the case of another possible value of  $E_x$  for the  $[2p_{3/2} \otimes 2_1^+]_{3/2}$ .<sup>5</sup> Later, a state at  $E_x = 2.011$  MeV was established to have  $J^\pi = \frac{3}{2}^-$  by electromagnetic-transition studies<sup>17, 18</sup> in agreement with the assignment from the  $^{62}\text{Ni}(^3\text{He}, d)^{63}\text{Cu}$  reaction.<sup>20</sup> Britton and Watson suggested that rather than the 1.55 MeV state, the 2.01 MeV state might have the configuration  $[2p_{3/2} \otimes 2_1^+]_{3/2}$ .<sup>20</sup>

In the present  $^{63}\text{Cu}(p, p')^{63}\text{Cu}$  experiment, transitions to six final states have been assigned to be  $L=2$  (Fig. 14). All these states are also excited

in the  $^{65}\text{Cu}(p, t)^{63}\text{Cu}$  reaction. Of these six transitions, the four leading to the states at 0.67, 0.96, 1.33, and 2.01 MeV have very similar angular distributions both in  $(p, p')$  (Fig. 8) and in  $(p, t)$  (Fig. 4). Therefore, the 0.67 ( $\frac{1}{2}^-$ ), 0.96 ( $\frac{5}{2}^-$ ), 1.33 ( $\frac{7}{2}^-$ ), and 2.01 MeV ( $\frac{3}{2}^-$ ) states are considered to be the members of the quartet  $2p_{3/2} \otimes 2_1^+$ .

The  $(p, p')$  angular distributions for the 1.41 and 1.55 MeV states are similar to one another, differing from the above-mentioned four states in the angular range from  $10^\circ$  through  $40^\circ$  c.m. (Fig. 8). This suggests a difference in the excitation mechanisms between these two states and the four states mentioned earlier. The 1.55 MeV state is excited by a mixed  $L=0+2$  transition in  $(p, t)$  (Fig. 6), as already mentioned. As pointed out in Sec. V A, this state has a substantial component  $[2p_{3/2} \otimes 0_2^+]_{3/2}$ , where  $0_2^+$  indicates the first excited  $0^+$  state at  $E_x = 2.05$  MeV in  $^{62}\text{Ni}$ . On the other hand, the fact that the 1.55 MeV state has a very small spectroscopic factor in the reaction  $^{62}\text{Ni}(^3\text{He}, d)^{63}\text{Cu}$  and decays mainly by an M1 transition<sup>4,18</sup> led Britton and Watson to suggest that it is a member of a doublet formed by coupling a  $2p_{1/2}$  proton to a one-phonon state.<sup>20</sup> If a low-lying  $\frac{3}{2}^-$  state has a large component of the form  $[2p_{3/2} \otimes 2_1^+]_{3/2}$  as a member of the quartet  $2p_{3/2} \otimes 2_1^+$ , it must have a substantial admixture of the component  $[2p_{3/2} \otimes 0_1^+]_{3/2}$  through the particle-core interactions, which means in turn a substantial spectroscopic factor in the reaction  $^{62}\text{Ni}(^3\text{He}, d)^{63}\text{Cu}$ .<sup>4,20</sup> This expectation is met by the 2.01 MeV state, but not by the 1.55 MeV state.<sup>20</sup> Thus, the properties of the 1.55 MeV state are quite different from those expected for the  $\frac{3}{2}^-$  member of the quartet  $2p_{3/2} \otimes 2_1^+$ . If the 1.55 MeV state has a substantial amplitude of the component  $[2p_{1/2} \otimes 2_1^+]_{3/2}$ , some other state must contain as its component the other member  $[2p_{1/2} \otimes 2_1^+]_{5/2}$  of the doublet  $2p_{1/2} \otimes 2_1^+$ . The similarity of the  $(p, p')$  angular distributions for the 1.41 and 1.55 MeV states (Fig. 8) suggests that the 1.41 MeV ( $\frac{5}{2}^-$ ) state has a substantial  $[2p_{1/2} \otimes 2_1^+]_{5/2}$  component. It may be that the absence of a bump around  $25^\circ$  c.m. in those  $(p, p')$  angular distributions indicates some effect of the interference between the pure core excitation  $\langle 62; 2_1^+ || \hat{Y}_2 || 2_1^+; 62 \rangle$  and the additional proton spin flip  $(2p_{3/2} - 2p_{1/2})$  accompanying the core excitations  $\langle 62; 2_1^+ || \hat{Y}_2 || 0_1^+; 62 \rangle$  and  $\langle 62; 2_1^+ || \hat{Y}_2 || 2_1^+; 62 \rangle$ .<sup>31</sup> Although the  $(p, t)$  angular distribution for the 1.41 MeV state is clearly  $L=2$ , it is somewhat different from the angular distributions for the 0.67, 0.96, 1.33, and 2.01 MeV states.

The identification of the 0.67 ( $\frac{1}{2}^-$ ), 0.96 ( $\frac{5}{2}^-$ ), 1.33 ( $\frac{7}{2}^-$ ), and 2.01 MeV ( $\frac{3}{2}^-$ ) states with the members of the quartet  $2p_{3/2} \otimes 2_1^+$ , and of the 1.41 ( $\frac{5}{2}^-$ )

and 1.55 MeV ( $\frac{3}{2}^-$ ) states with the members of the doublet  $2p_{1/2} \otimes 2_1^+$  is strengthened by the  $B(E2)$  values derived from the most recent  $\gamma$ -decay data.<sup>18</sup>

Because of the mixing by the particle-core interactions, the proton single-particle components  $[2p_{3/2} \otimes 0_1^+]_{3/2}$ ,  $[2p_{1/2} \otimes 0_1^+]_{1/2}$ , and  $[1f_{5/2} \otimes 0_1^+]_{5/2}$  are present, respectively, in the 2.01 MeV ( $\frac{3}{2}^-$ ) state, 0.67 MeV ( $\frac{1}{2}^-$ ) state, and 0.96 and 1.41 MeV ( $\frac{5}{2}^-$ ) states, with the spectroscopic factors measured in the  $^{62}\text{Ni}(^3\text{He}, d)^{63}\text{Cu}$  reaction.<sup>20</sup> If the  $Z=28$  shell closure is assumed to be complete, as is usually done in the particle-core-coupling calculations, there is no room for the proton single-particle component  $[1f_{7/2} \otimes 0_1^+]_{7/2}$ . If the 1.33 MeV ( $\frac{7}{2}^-$ ) state is thus assumed to be the pure excited-core state  $[2p_{3/2} \otimes 2_1^+]_{7/2}$ ,<sup>32</sup> the transition amplitude involving the reduced matrix element (3) or (3') vanishes in the transition to this state. Further, if the transition amplitude involving (2) or (2') is far smaller than that involving (1) or (1'), then the transition to the 1.33 MeV ( $\frac{7}{2}^-$ ) state is made only by the transition amplitude involving the reduced matrix element (1) or (1') which connects the component  $[2p_{3/2} \otimes 0_1^+]_{3/2}$  of the ground state of  $^{63}\text{Cu}$  or  $^{65}\text{Cu}$  to the pure configuration  $[2p_{3/2} \otimes 2_1^+]_{7/2}$ . Thus, the same matrix element is involved in the above transition and the transition to the  $2_1^+$  state in  $^{62}\text{Ni}$  in the "core" reaction  $^{62}\text{Ni}(p, p')^{62}\text{Ni}$  or  $^{64}\text{Ni}(p, t)^{62}\text{Ni}$ . In such a case, the ratio of the cross section for the transition to a pure excited-core state  $[nlj \otimes I]_J$  with spin  $J$  to that for the transition to the corresponding collective state with spin  $I$  in the "core" reaction is equal to

$$R = S \frac{2J+1}{(2j+1)(2I+1)}, \quad (6)$$

where  $n, l, j$  denote a relevant proton single-particle orbital, and  $S$  denotes the spectroscopic factor for the proton single-particle component  $[nlj \otimes 0_1^+]_J$  in the ground state of the target nucleus. Using  $J = \frac{7}{2}$ ,  $j = \frac{3}{2}$ ,  $I = 2$ , and  $S = 0.75$  from the  $^{62,64}\text{Ni}(^3\text{He}, d)^{63,65}\text{Cu}$  work,<sup>20</sup> the ratio  $R = 0.30$  is obtained. For the  $^{63}\text{Cu}(p, p')^{63}\text{Cu}$ , the ratio derived from the present data and the  $^{62}\text{Ni}(p, p')^{62}\text{Ni}$  data<sup>24</sup> is  $0.31 \pm 0.06$ , which is in agreement with the prediction of the model.<sup>33</sup> For the  $^{65}\text{Cu}(p, t)^{63}\text{Cu}$  reaction, the ratio derived from the present data and the  $^{64}\text{Ni}(p, t)^{62}\text{Ni}$  data<sup>15</sup> is  $0.32 \pm 0.06$ , which is again in agreement with the model prediction. Thus, the assumption that the transition amplitude involving (2) or (2') is far smaller than that involving (1) or (1') is consistent with the experimental data. The assumption requires the amplitude of the component  $[2p_{3/2} \otimes 2_1^+]_{3/2}$  to be far smaller than that of the component  $[2p_{3/2} \otimes 0_1^+]_{3/2}$  in the ground state of  $^{63}\text{Cu}$  or  $^{65}\text{Cu}$ , unless (2) or (2') is far smaller than (1) or (1'). The reduced matrix

element (2) is of the same order of magnitude as (1).<sup>2,5</sup>

The 2.06 MeV state is excited by an  $L=2$  ( $p, t$ ) transition, but is missing in the ( $p, p'$ ) (Fig. 14). This state was also observed in  $\gamma$ -ray work<sup>17,18</sup> and in a  $^{62}\text{Ni}(^3\text{He}, d)^{63}\text{Cu}$  experiment.<sup>20</sup> The  $j$  dependence of the  $l=1$  ( $^3\text{He}, d$ ) angular distribution was used to assign  $J^\pi = \frac{1}{2}^-$  to the state,<sup>20</sup> while the  $\gamma$ -ray work did not exclude the possibility of  $J^\pi = \frac{3}{2}^-$ .<sup>17,18</sup> If the assignment of  $J^\pi = \frac{1}{2}^-$  is correct, the state is certainly the partner of the 0.67 MeV ( $\frac{1}{2}^-$ ) state in the particle-core mixing, just as the 2.01 MeV ( $\frac{3}{2}^-$ ) state is the partner of the ground state. The absence of the 2.06 MeV state in the ( $p, p'$ ) spectrum is somewhat puzzling, but an "accidental" cancellation can occur between transition amplitudes involving the reduced matrix elements (1), (2), and (3).

In summary, the present ( $p, p'$ ) and ( $p, t$ ) data, together with previous experimental evidence,<sup>18,20</sup> establish that the states at  $E_x = 0.67, 0.96, 1.33$  and 2.01 MeV have the properties expected of the  $\frac{1}{2}^-$ ,  $\frac{3}{2}^-$ ,  $\frac{7}{2}^-$ , and  $\frac{3}{2}^-$  members of the quartet  $2p_{3/2} \otimes 2_1^+$ . The states at  $E_x = 1.41$  and 1.55 MeV have most of the properties of the  $\frac{5}{2}^-$  and  $\frac{3}{2}^-$  members of the doublet  $2p_{1/2} \otimes 2_1^+$ .

### 2. Octupole multiplets

A quartet-plus-doublet pattern is observed for the octupole states in  $^{63}\text{Cu}$  (Fig. 15). The 3.32, 3.48, 3.72, and 3.84 MeV states have been identified as the members of the quartet  $2p_{3/2} \otimes 3_1^-$ , and the 3.81 and 3.89 MeV states as the doublet  $2p_{1/2} \otimes 3_1^-$ , where  $3_1^-$  denotes the  $3^-$  state at  $E_x = 3.75$  MeV in  $^{62}\text{Ni}$ .<sup>27</sup> The relative cross sections for the six states have been reproduced by the use of a new ground-state wave function.<sup>27</sup> The major features of the wave function are the small size of the component  $[2p_{3/2} \otimes 2_1^+]_{3/2}$  and the large size of the component  $[2p_{1/2} \otimes 2_1^+]_{3/2}$ .

A comparative analysis of the angular distributions for the ground-state transitions in the reactions  $^{65}\text{Cu}(p, t)^{63}\text{Cu}$  and  $^{64}\text{Ni}(p, t)^{62}\text{Ni}$  (Ref. 16) also suggests that the  $[2p_{3/2} \otimes 2_1^+]_{3/2}$  component in the ground state of  $^{63}\text{Cu}$  is small. Further evidence from the properties of the 1.33 MeV ( $\frac{7}{2}^-$ ) state was discussed above. On the other hand, the large size of the component  $[2p_{1/2} \otimes 2_1^+]_{3/2}$  makes possible the core excitation of doublets  $2p_{1/2} \otimes 2_1^+$ ,  $3_1^-$ , etc., with observable strengths.

The octupole state at  $E_x = 2.51$  MeV (Fig. 15) will be discussed below.

### 3. Hexadecapole multiplets

The 2.21, 2.34, 2.54, and 2.68 MeV states, observed in both the reactions  $^{65}\text{Cu}(p, t)^{63}\text{Cu}$  and

$^{63}\text{Cu}(p, p')^{63}\text{Cu}$ , are considered to be members of the quartet  $[2p_{3/2} \otimes 4_1^+]_{5/2, 7/2, 9/2, 11/2}$  formed by the coupling of the  $2p_{3/2}$  proton orbital with the  $4_1^+$  state at  $E_x = 2.33$  MeV in  $^{62}\text{Ni}$  (Fig. 16). An analogy with the case of the octupole states<sup>27</sup> leads to the identification of the 2.85 and 2.88 MeV states observed in the  $^{65}\text{Cu}(p, t)^{63}\text{Cu}$  with the members of the doublet  $[2p_{1/2} \otimes 4_1^+]_{7/2, 9/2}$ . The 2.21 and 2.34 MeV states seem to be identical with the 2.2080 and 2.3365 MeV states with  $J^\pi = \frac{9}{2}^-$  and  $\frac{5}{2}^-$  (Table I) reported in the  $\gamma$ -ray work of Papadopoulos *et al.*<sup>18</sup> The 2.54 MeV state cannot be identified with the 2.5358 MeV state (Table I) of Papadopoulos *et al.*, if their assignment of  $J^\pi = \frac{5}{2}^-$  to both the 2.3365 and 2.5358 MeV states is correct. A state is reported in the literature at  $E_x = 2.543$  MeV along with the 2.5358 MeV state.<sup>34</sup>

The 2.68 MeV state is the strongest hexadecapole state in both the ( $p, p'$ ) and ( $p, t$ ) reactions (Fig. 16). This indicates that the state is the  $J^\pi = \frac{11}{2}^-$  member of the quartet  $2p_{3/2} \otimes 4_1^+$ . The members of the quartet are excited coherently by the two amplitudes involving the reduced matrix elements (4) and (5) in ( $p, p'$ ), or the reduced matrix elements (4') and (5') in ( $p, t$ ). The  $J^\pi = \frac{11}{2}^-$  member is expected to be least mixed with other configurations because of its high spin. If the 2.68 MeV state is assumed to be the pure  $[2p_{3/2} \otimes 4_1^+]_{11/2}$  state, and if the transition amplitude involving the reduced matrix element (5) or (5') is far smaller than that involving (4) or (4'), then formula (6) is applicable. The ratio of the cross section for the 2.68 MeV state to that for the 2.33 MeV state in  $^{62}\text{Ni}$  is predicted to be  $R = 0.25$ , by substituting  $S = 0.75$ ,<sup>20</sup>  $J = \frac{11}{2}$ ,  $j = \frac{3}{2}$ , and  $I = 4$  into (6). The experimental value of the ratio in the ( $p, p'$ ), derived from the present data (Fig. 10) and the  $^{62}\text{Ni}(p, p')^{62}\text{Ni}$  data,<sup>24</sup> is  $0.26 \pm 0.05$ , in agreement with the predicted value.<sup>33</sup> The experimental value in the ( $p, t$ ), derived from the present data (Fig. 5) and the  $^{64}\text{Ni}(p, t)^{62}\text{Ni}$  data,<sup>15</sup> is  $0.28 \pm 0.05$ , also in agreement with the predicted value within the experimental error. Thus, the identification of the 2.68 MeV state with the  $J^\pi = \frac{11}{2}^-$  member of the quartet  $2p_{3/2} \otimes 4_1^+$  is reasonable. It is further consistent with the fact that the state is missing in  $^{62}\text{Ni}(^3\text{He}, d)$  experiments<sup>19,20</sup> and has never been found in  $\gamma$ -ray work that has so far been able to detect only low-spin states.<sup>17,18</sup>

The 3.19, 3.21, 3.23, and 3.26 MeV states are considered to be members of the quartet corresponding to the  $4_3^+$  state at  $E_x = 3.27$  MeV in  $^{62}\text{Ni}$  (Fig. 16). While their extremely close spacing might suggest a weak-coupling situation, paradoxically these transitions carry only a small fraction of the strength of the "core" transition to the 3.27 MeV ( $4_3^+$ ) state in the  $^{64}\text{Ni}(p, t)^{62}\text{Ni}$  reaction

(Fig. 16).<sup>15</sup> There seems to be a large amount of mixing with other configurations. The state at  $E_x = 3.38$  MeV is a candidate for the doublet  $[2p_{1/2} \otimes 4_3^+]_{7/2, 9/2}$ . In view of the above-mentioned quartet-plus-doublet pattern of the states corresponding to the 2.33 MeV ( $4_1^+$ ) state of the core, the extremely close spacing of the members of the quartet  $2p_{3/2} \otimes 4_3^+$  suggests the possibility that the 3.38 MeV state may be the unresolved doublet  $[2p_{1/2} \otimes 4_3^+]_{7/2, 9/2}$ .

#### 4. Other states

Not all the states observed in the present experiment belong to excited-core multiplets. The 1.86, 2.08, 2.09, and 2.41 MeV states are excited by mixed  $L = 2 + 4$  transitions (Table I). The  $L$  assignment is consistent with the spins and parities of these states. These states do not belong to particular multiplets. They may arise through a mixing between multiplets with different  $L$ 's within the framework of the particle-core-coupling picture, but the persistent occurrence of a quartet-plus-doublet pattern for each of the  $2_1^+$ ,  $3_1^-$ , and  $4_1^+$  states of the core implies that such mixing is weak. More probably they correspond to microscopic configurations that are beyond the scope of the particle-core-coupling picture. For example, the  $Z = 28$  shell closure is not exact, and proton configuration  $(2p_{3/2})^2(1f_{7/2})^{-1}$  can form states with  $J^\pi = \frac{7}{2}^-$  or  $\frac{5}{2}^-$ . Multistep processes may be important, too, in the excitation of complicated states.

The very strong octupole transition in the  $^{63}\text{Cu}(p, p')^{63}\text{Cu}$  to the 2.51 MeV state is not understandable as a simple core excitation (Fig. 15). The state is to be identified with the one observed in  $^{62}\text{Ni}(^3\text{He}, d)^{63}\text{Cu}$  experiments and assigned to be a predominantly proton-single-particle state  $[1g_{9/2} \otimes 0_1^+]_{19/2}$ ,<sup>19,20</sup> since no other positive-parity state is known in the vicinity of  $E_x = 2.51$  MeV. The large cross section for the transition to the predominantly single-particle state is a puzzle. Klaasse and Paar pointed out a possibility that the interference between the octupole proton-single-particle transition  $2p_{3/2} - 1g_{9/2}$  and processes involving the virtual excitation of the  $3_1^-$  state of the core can produce a large cross section.<sup>35</sup> A quantitative solution of this puzzle remains a task for future theoretical studies.

#### C. Energy dependence of the $^{63}\text{Cu}(p, p')^{63}\text{Cu}$ reaction

The above-mentioned difference between the  $L = 2$  ( $p, p'$ ) angular distributions for the quartet states and for the doublet states (Fig. 8) has been observed for the first time in the present experiment at  $E_p = 40$  MeV. In order to establish that the

effect is due to a difference in the reaction mechanism corresponding to a difference in the nuclear structure, it is necessary to study the energy dependence of the proton inelastic scattering by  $^{63}\text{Cu}$  and to check the stability of the difference.

In the low-energy region where the previous experiments<sup>6,9,12</sup> on the  $^{63}\text{Cu}(p, p')^{63}\text{Cu}$  reaction were performed, the mechanisms of proton inelastic scattering seem to be more complicated than at higher energies. An "anomalous" difference was observed between the angular distribution for the 0.67 MeV ( $\frac{1}{2}^-$ ) state and those for the 0.96 ( $\frac{5}{2}^-$ ) and 1.33 MeV ( $\frac{7}{2}^-$ ) states,<sup>12</sup> and there were some controversies about the apparent "final-state-spin dependence" in proton inelastic scattering.<sup>12,36-38</sup> No effect that amounts to a "final-state-spin dependence" is observed, however, at  $E_p = 40$  MeV in the present experiment (Fig. 8), which shows that the above "anomaly" exists only in a limited low-energy region. Also, the angular distribution for the 1.55 MeV ( $\frac{3}{2}^-$ ) state is rather flat at  $E_p = 11$  MeV,<sup>6</sup> indicating the existence of complicated mechanisms.

Although the reaction mechanism of proton inelastic scattering is simpler at higher energies, effects beyond the scope of the single-step core-excitation model are naturally expected to occur. Observable changes in the angular distribution shape can be produced, for example, by the interference between the proton-single-particle excitation and the dominant core excitation, or by the interference between the first-order (single-step) process and higher-order (multistep) processes. The differences among the forward parts of the experimental  $L = 2$  angular distributions (Fig. 8) contain information on the reaction mechanisms.

Not only the angular distribution shape, but also relative cross sections for different states provide information on reaction mechanisms. If only the single-step core excitation is possible, the relative cross sections for transitions of one and the same multipole  $L$  are energy independent, even if there is a particle-core mixing. This is due to the energy independence of the relative values of the reduced matrix elements involved in the single-step core excitation of a given multipole  $L$ . For example, referring to the case of  $L = 2$ , the relative values of the reduced matrix elements (1), (2), and (3) are energy independent, because (1), (2), and (3) are matrix elements of  $\hat{Y}_2$ , which is the quadrupole moment operator multiplied by a constant. Thus, any deviation from energy independence of the experimental relative cross sections for the same multipole  $L$  is evidence of more complicated reaction mechanisms. The relative cross sections for different multipoles  $L$  depend on energy, since the multiplicative con-



starts for different multipole moment operators have different energy dependences.

The statements in the above paragraph apply to the  $(p, t)$  reaction as well as to the  $(p, p')$ . Table III shows the experimental energy dependence of the relative cross sections for  $L=2$  transitions to the four lowest excited states in the  ${}^{63}\text{Cu}(p, p'){}^{63}\text{Cu}$  and  ${}^{65}\text{Cu}(p, t){}^{63}\text{Cu}$  reactions. A remarkable deviation from energy independence is observed for the  $(p, p')$  transition to the 1.41 MeV ( $\frac{5}{2}^-$ ) state, suggesting the existence of many excitation mechanisms.

#### D. Apparent weak-coupling pattern observable in transfer reactions

Since the earliest  $(p, t)$  experiments on odd-proton nuclei,<sup>10,11,25,39</sup> there has been rapid progress in the application of transfer reactions to the study of particle-core coupling.<sup>26,40-42</sup> The information obtainable by transfer reactions has a unique feature in contrast to that obtainable by inelastic scattering. To be specific, the case of the reaction  ${}^{65}\text{Cu}(p, t){}^{63}\text{Cu}$  is considered and it is assumed (fictitiously of course) that the ground state of  ${}^{65}\text{Cu}$  is simply a pure proton-single-particle state  $[2p_{3/2} \otimes 0^+]_{3/2}$ . Then, only one transition amplitude which involves a reduced matrix element of the type (1') or (4') would be different from zero for each collective state of the core. The  ${}^{65}\text{Cu}(p, t){}^{63}\text{Cu}$  reaction would not populate excited-core doublets  $[2p_{1/2} \otimes 2^+]_{3/2, 5/2}$ ,  $[2p_{1/2} \otimes 3^+]_{5/2, 7/2}$ , and  $[2p_{1/2} \otimes 4^+]_{7/2, 9/2}$ . Only the quartets  $[2p_{3/2} \otimes 2^+]_{1/2, 3/2, 5/2, 7/2}$ ,  $[2p_{3/2} \otimes 3^+]_{3/2, 5/2, 7/2, 9/2}$ , and  $[2p_{3/2} \otimes 4^+]_{5/2, 7/2, 9/2, 11/2}$  would be observed in  ${}^{63}\text{Cu}$ . There would be no interference effect in the core-excitation process. The relative cross sections for the members of a quartet would follow the  $(2J+1)$  rule,<sup>6-8,42</sup> even though there is a substantial mixing of the members with other configurations, provided that the mixing were uniform for the quartet members. Of course, the

absolute cross sections for the quartet members would be smaller than in the case of no mixing in  ${}^{63}\text{Cu}$ . Still the ratio between the sum of the absolute cross sections for the quartet members and the absolute cross section for the ground-state transition would indicate qualitatively a weak-coupling situation, as is often observed,<sup>10,41,42</sup> since the latter is smaller, too, than it should be in the case of no mixing. Thus, there would appear a simple weak-coupling pattern, which is deceptive in view of the real particle-core-coupling situation in  ${}^{63}\text{Cu}$ . In short, in spite of a complicated particle-core-coupling structure, a simple weak-coupling pattern may appear in transfer reaction data because of the simplicity of the ground state of the target nucleus. For example, "unexpected weak-coupling behavior in  ${}^{17}\text{O}({}^6\text{Li}, d){}^{21}\text{Ne}$ "<sup>42</sup> may arise because of the simple particle-core structure of the ground state of  ${}^{17}\text{O}$ , even if the particle-core mixing is large in  ${}^{21}\text{Ne}$ .

There is another source of the deceptive appearance of the weak-coupling pattern in transfer reactions. It is easily seen that the argument in the preceding paragraph can be generalized: A weak-coupling pattern appears if the particle-core mixing is uniform, even though large in a nucleus, and if the core excitation is effected by only one transition amplitude involving a reduced matrix element of the type (1) or (1'). The latter assumption is satisfied even if the ground-state wave function of the target nucleus is not as simple as in the preceding paragraph, if matrix elements of types (2) and (3) [or (2') and (3')] are far smaller than the matrix element of type (1) or (1'). This is impossible, however, in inelastic scattering, where the reduced matrix element (3) is always equal in magnitude to (1), and (2) is generally not small compared with (1).<sup>2,5</sup> In the  $(p, t)$  reaction, the reduced matrix element (3') may be far smaller than (1') (for example, toward the end of a

TABLE III. Incident proton energy dependence of the relative cross sections for the four lowest excited states in  ${}^{63}\text{Cu}$ . Summed cross sections are normalized to 1.00 for the 1.33 MeV state.

| $E_x$ | ${}^{65}\text{Cu}(p, t){}^{63}\text{Cu}$ |                     | 52 MeV <sup>c</sup> | ${}^{63}\text{Cu}(p, p'){}^{63}\text{Cu}$ |                     |
|-------|------------------------------------------|---------------------|---------------------|-------------------------------------------|---------------------|
|       | 19.5 MeV <sup>a</sup>                    | 40 MeV <sup>b</sup> |                     | 17.5 MeV <sup>d</sup>                     | 40 MeV <sup>b</sup> |
| 0.67  | 0.18                                     | 0.16                | 0.18                | 0.29                                      | 0.23                |
| 0.96  | 0.46                                     | 0.43                | 0.46                | 1.00                                      | 0.91                |
| 1.33  | 1.00                                     | 1.00                | 1.00                | 1.00                                      | 1.00                |
| 1.41  | 0.09                                     | 0.10                | 0.07                | 0.16                                      | 0.08                |

<sup>a</sup> Reference 11.

<sup>b</sup> Present work.

<sup>c</sup> Reference 10.

<sup>d</sup> Reference 9.

large neutron shell), and (2') seems to be considerably smaller than (1').<sup>11</sup> Therefore, even if the particle-core structure of the ground state of the target nucleus is not simple, a weak-coupling pattern may appear in transfer-reaction data in some mass regions.

The above arguments demonstrate the importance of the comparative study of core excitations in the same nucleus by the inelastic scattering and transfer reactions. While it is dangerous to conclude the existence of a weak-coupling situation only on the basis of transfer-reaction data, they give unique clues for unraveling generally more complicated information from the inelastic scattering.

In the present case of the  $^{63}\text{Cu}(p, p')^{63}\text{Cu}$  and  $^{65}\text{Cu}(p, t)^{63}\text{Cu}$  reactions qualitatively similar spectra are observed in the inelastic scattering and the transfer reaction for the  $L = 2$  and  $L = 4$  excitations. This is readily understandable. First, the ground-state wave functions of  $^{63}\text{Cu}$  and  $^{65}\text{Cu}$  are similar. Secondly, at the middle of the neutron  $1f-2p$  shell, the reduced matrix element (3') is close to (1').<sup>11</sup> The difference between the ratio of (2) to (1) and the ratio of (2') to (1') is the major source of differences between the  $^{63}\text{Cu}(p, p')^{63}\text{Cu}$  and the  $^{65}\text{Cu}(p, t)^{63}\text{Cu}$  in the relative cross sections for the members of the  $L = 2$  multiplets (Fig. 14).

## VII. SUMMARY AND CONCLUSIONS

It has been shown that a quartet-plus-doublet pattern exists consistently for the groups of states located at excitation energies near to the  $2_1^+$ ,  $3_1^-$ , and  $4_1^+$  states of the core nucleus  $^{62}\text{Ni}$ . The quartet-plus-doublet interpretation which was worked out quantitatively for the octupole excited-core states<sup>27</sup> seems also to be applicable to the quadrupole and hexadecapole excited-core states, at least qualitatively. The present data for the reactions  $^{63}\text{Cu}(p, p')^{63}\text{Cu}$  and  $^{65}\text{Cu}(p, t)^{63}\text{Cu}$ , combined with previous data from the  $^{62}\text{Ni}(^3\text{He}, d)^{63}\text{Cu}$  reaction<sup>20</sup> and  $\gamma$  decay,<sup>18</sup> have clarified the situation regarding the low-lying quadrupole states, making it possible to identify the members of the quartet  $2p_{3/2} \otimes 2_1^+$

and the doublet  $2p_{1/2} \otimes 2_1^+$  and to distinguish them from other states of more complicated nature such as the 1.86 MeV ( $\frac{7}{2}^-$ ) state. The hexadecapole multiplets have been discovered for the first time. The persistent occurrence of the quartet-plus-doublet pattern is evidence that the mixing between different multiplets (in particular, multiplets corresponding to different collective states of the core) is weak, and that the component  $[2p_{1/2} \otimes 2_1^+]_{3/2}$  exists in the ground states of  $^{63}\text{Cu}$  and  $^{65}\text{Cu}$  with a considerable amplitude.

Differences between the relative cross sections for the members of a multiplet in  $^{63}\text{Cu}(p, p')^{63}\text{Cu}$  and  $^{65}\text{Cu}(p, t)^{63}\text{Cu}$  are attributed to differences between the relative values of the core-excitation matrix elements in the two reactions, as well as to differences between the ground-state wave functions of  $^{63}\text{Cu}$  and  $^{65}\text{Cu}$ . These arguments can be generalized to apply to other nuclei and to other reactions. Inelastic scattering and transfer reactions thus give different information about the particle-core-coupling structure of the same final nucleus, because of the different relative values of the core-excitation matrix elements and the different particle-core wave functions of the ground states of the target nuclei. The comparative study of the core excitations by the inelastic scattering and the transfer reaction is therefore very important.

The present experimental study has created a coherent qualitative picture of the particle-core coupling in  $^{63}\text{Cu}$ , which is supported by a large amount of experimental evidence. The richness of high-quality experimental data on  $^{63}\text{Cu}$  that have been accumulated in recent years<sup>17,18,20,27</sup> should hopefully encourage a comprehensive theoretical investigation to try to achieve a better quantitative understanding of this nucleus.

## VIII. ACKNOWLEDGMENTS

The authors would like to thank R. G. Markham for his help with the experiment. This material is based upon work supported by the National Science Foundation under Grant No. Phy. 78-22696.

\*Present address: Kernfysisch Versneller Instituut, University of Groningen, Groningen, The Netherlands.

<sup>1</sup>A. de-Shalit, Phys. Rev. **122**, 1530 (1961).

<sup>2</sup>V. K. Thankappan and W. W. True, Phys. Rev. **137**, B793 (1965).

<sup>3</sup>A. Bohr and B. R. Mottelson, *Nuclear Structure* (Benjamin, Reading, Mass., 1975), Vol II.

<sup>4</sup>V. Paar, Nucl. Phys. **A147**, 369 (1970).

<sup>5</sup>J. L. de Jager and E. Boeker, Nucl. Phys. **A216**, 349 (1973).

<sup>6</sup>F. Perey, R. J. Silva, and G. R. Satchler, Phys. Lett. **4**, 25 (1963).

<sup>7</sup>G. Bruge, J. C. Faivre, M. Barloutaud, H. Faraggi, and J. Saudinos, Phys. Lett. **7**, 203 (1963).

<sup>8</sup>B. G. Harvey, J. R. Meriwether, A. Bussiere, and D. J. Horen, Nucl. Phys. **70**, 305 (1965).

<sup>9</sup>A. L. McCarthy and G. M. Crawley, Phys. Rev. **150**, 935 (1966).

<sup>10</sup>Y. Iwasaki, M. Sekiguchi, F. Soga, and N. Takahashi, Phys. Rev. Lett. **29**, 1528 (1972).

- <sup>11</sup>R. G. Markham and H. W. Fulbright, Nucl. Phys. A203, 244 (1973).
- <sup>12</sup>J. C. Legg and J. L. Yntema, Phys. Rev. Lett. 22, 1005 (1969).
- <sup>13</sup>R. G. Markham and R. G. H. Robertson, Nucl. Instrum. Methods 129, 131 (1975).
- <sup>14</sup>Y. Iwasaki, T. Murata, T. Tamura, and Y. Nogami, Phys. Rev. C 13, 556 (1976).
- <sup>15</sup>D. H. Kong-A-Siou and H. Nann, Phys. Rev. C 11, 1681 (1975).
- <sup>16</sup>Y. Iwasaki (unpublished).
- <sup>17</sup>C. P. Swann, Phys. Rev. C 13, 1104 (1976).
- <sup>18</sup>C. T. Papadopoulos, A. G. Hartas, P. A. Assimakopoulos, G. Andritsopoulos, and N. H. Gangas, Phys. Rev. C 15, 1987 (1977).
- <sup>19</sup>A. G. Blair, Phys. Rev. 140, B648 (1965).
- <sup>20</sup>R. M. Britton and D. L. Watson, Nucl. Phys. A272, 91 (1976).
- <sup>21</sup>P. D. Kunz, University of Colorado (unpublished).
- <sup>22</sup>F. D. Becchetti, Jr. and G. W. Greenlees, Phys. Rev. 182, 1190 (1969).
- <sup>23</sup>N. Lingappa and G. W. Greenlees, Phys. Rev. C 2, 1329 (1970); B. M. Preedon, C. R. Gruhn, T. Y. T. Kuo, and C. J. Maggiore, *ibid.* 2, 166 (1970); C. R. Gruhn, T. Y. T. Kuo, C. J. Maggiore, and B. M. Preedon, *ibid.* 6, 944 (1972).
- <sup>24</sup>K. M. Thompson, Ph.D. thesis, Michigan State University, 1969 (unpublished).
- <sup>25</sup>K. K. Seth, H. Ohnuma, T. Suehiro, S. Yamada, and S. Takeda, Phys. Rev. Lett. 30, 132 (1973).
- <sup>26</sup>K. K. Seth, A. Saha, W. Stewart, W. Benenson, W. A. Lanford, H. Nann, and B. H. Wildenthal, Phys. Lett. 49B, 157 (1974).
- <sup>27</sup>Y. Iwasaki, G. M. Crawley, R. G. Markham, J. E. Finck, and J. H. Kim, Phys. Rev. C 20, 861 (1979).
- <sup>28</sup>G. E. Brown, *Unified Theory of Nuclear Models and Forces* (North-Holland, Amsterdam, 1971).
- <sup>29</sup>M. Bouten and P. van Leuven, Nucl. Phys. 32, 499 (1962); 76, 479 (1966); W. P. Beres, *ibid.* 68, 49 (1965); 75, 255 (1966); D. Lerner, Phys. Rev. C 2, 522 (1970); J. M. G. Gomez, Nucl. Phys. A173, 537 (1971); B. Castel, I. P. Johnstone, B. P. Singh, and K. W. C. Stewart, Can. J. Phys. 50, 1630 (1972).
- <sup>30</sup>R. G. Markham and H. W. Fulbright, Report No. UR-NSRL-41.
- <sup>31</sup>The pure core excitation of the members of the doublet  $2p_{1/2} \otimes 2_1^+$  is possible only by the reduced matrix element (2) since the  $2p_{1/2}$  orbital exists in the ground state only in the form  $[2p_{1/2} \otimes 2_1^+]_{3/2}$ .
- <sup>32</sup>A small component of the form  $[1f_{5/2} \otimes 2_1^+]_{7/2}$  is possible in the 1.33 MeV ( $\frac{7}{2}^-$ ) state.
- <sup>33</sup>The accuracy in this kind of comparison is limited by the rather large error (about 10 to 15%) inherent in each measurement of the absolute cross section.
- <sup>34</sup>R. L. Auble, Nucl. Data Sheets 14, 119 (1975).
- <sup>35</sup>A. A. C. Klaasse and V. Paar, Nucl. Phys. A297, 45 (1978).
- <sup>36</sup>M. Dost, C. Glashauser, and C. F. Haynes, Nucl. Phys. A183, 285 (1972).
- <sup>37</sup>R. Reif and R. Schmidt, Phys. Lett. 52B, 163 (1974).
- <sup>38</sup>W. G. Love and F. Todd Baker, Phys. Rev. Lett. 35, 1219 (1975).
- <sup>39</sup>K. A. Erb and T. S. Bhatia, Phys. Rev. C 7, 2500 (1973).
- <sup>40</sup>R. M. Del Vecchio, R. A. Naumann, J. R. Duray, H. Hubel, and W. W. Daehnick, Phys. Rev. C 12, 69 (1975); R. M. Del Vecchio, I. C. Oelrich, and R. A. Naumann, *ibid.* 12, 845 (1975); A. W. Kuhfeld and N. M. Hintz, Nucl. Phys. A247, 152 (1975); H. Nann, B. H. Wildenthal, A. Saha, and K. K. Seth, Phys. Rev. Lett. 35, 609 (1975).
- <sup>41</sup>I. C. Oelrich, K. Krien, R. M. Del Vecchio, and R. A. Naumann, Phys. Rev. C 14, 563 (1976).
- <sup>42</sup>N. Anantaraman, H. E. Gove, J. Toke, and H. T. Fortune, Phys. Lett. 74B, 199 (1978).